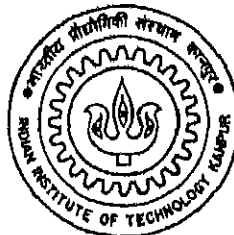


# PLANNING AND DESIGN OF NATIONAL COMMAND COMPLEX

by  
CAPT SANJAY SHARMA



DEPARTMENT OF CIVIL ENGINEERING  
INDIAN INSTITUTE OF TECHNOLOGY KANPUR  
APRIL, 1995

CE

1995

M

SHA

PLA

# PLANNING AND DESIGN OF NATIONAL COMMAND COMPLEX

A Thesis Submitted  
in Partial Fulfillment of the Requirements  
for the Degree of

MASTER OF TECHNOLOGY

*by*

*Capt Sanjay Sharma*

to the  
DEPARTMENT OF CIVIL ENGINEERING  
INDIAN INSTITUTE OF TECHNOLOGY KANPUR  
April, 1995

26 APR 1996  
CENTRAL JAIL  
UTTAR KANPUR  
Am. No. A. 121377

CE-1995-M-SHA-PLA



A121377

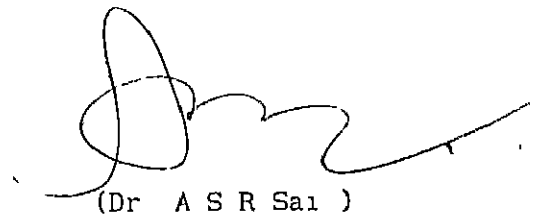
*Dedicated*

*to*

*My parents and wife*

## CERTIFICATE

It is certified that the work contained in the thesis entitled,  
" PLANNING DESIGN OF NATIONAL COMMAND COMPLEX ", has been carried out by  
Capt Sanjay Sharma under my supervision and this work has not been  
submitted elsewhere for the award of a degree.



(Dr A S R Sai )

Professor

Department of Civil Engineering

I I T Kanpur

## ACKNOWLEDGEMENTS

It gives me profound pleasure to express my deep gratitude to my supervisor Dr A.S.R Sai, Professor of Civil Engineering for his invaluable guidance and wise counsel. He has always been a constant source of encouragement for me.

I am extremely grateful to my most beloved teacher Dr C.V R Murty who gave me the required orientation whenever needed

I wish to place on records my sincere thanks to Lt Col G H R Naidu and the officers of NBC cell and R & D (Engrs), Pune for providing me a practical outlook on this subject.

I am thankful to Prof Mrs Sai for her warm motherly affection throughout my stay at I I T Kanpur.

I am also grateful to my friends Amit, Manish, Arvind, S B Singh, Joydeep, Samarth, Kumar and Ashok for helping me on various technical and non technical aspects.

Last but not the least, I am indebted to my wife Abha and my daughter Palak for their suffering due to my absence from home for most of the time.

*Sanjay*

## CONTENTS

Title	Page Number
Certificate	ii
Acknowledgements	iii
Contents	iv
List of Figures	viii
List of Tables	x
Symbols	xi
Abstract	xiv
<b>Chapter - I      Introduction</b>	<b>1</b>
1.1    General	1
1.2    Philosophy of Warfare	1
1.3    Nuclear Environment	2
1.4    Protective Shelters	3
1.5    Scope of the Present Study	4
1.6    Aim	5
1.7    General Standard Qualitative Requirements	6
1.8    Planning and Layout	6
1.9    Organization of the Thesis	9
<b>Chapter - II    Review of Literature</b>	<b>10</b>
2.1      Scope	10
2.2      General	10
2.3      Blast and Shock Effects	11
2.3.1      Over Pressure and Dynamic Pressure	14
2.3.2      Pressure Time Histories	16
2.3.3      Approximate Analysis	17
2.3.4      Dynamic pressure	17

2 4	Crater Effects	19
2 5	Ground Motions	20
2 6	Radiation Effects	22
2.6.1	$\alpha$ and $\beta$ Radiations	22
2.6.2	$\gamma$ - Rays	23
2.6 3	Neutron Radiation	32
2 7	Thermal Radiation	34
2.7 1	Technical Aspects of Thermal Radiation	35
2 8	Other Effects	37
2.8.1	Electromagnetic Pulse Effects	38
2.8.2	Derbis	38
2 8.3	Dust	39
2.8.4	Fires	39
2 9	Threat Perception and Reliability Analysis	39
2 10	Blast Loading and Soil Arching Effects	40
2.10 1	Air Blast loading on Below Ground Structures	41
2.10.2	Shallow Buried Structures	42
2.10.3	Soil Arching	42
2.10.4	Shallow Buried Rectangular Structures	46
2.10.5	Shallow Buried Shells	48
2.10.6	Mounded Structures	52
2.10.7	Surface Flush Structures	54
2.11	Analysis and Design	55
2.11.1	Static Analysis	56
2.11.2	Dynamic Analysis	57

2 11 3	Design	59
2 12	Comments on Literature Review	60
<b>Chapter - III</b>	<b>Design and Analysis</b>	<b>64</b>
3 1	Proposed Algorithm	64
3 2	Parametric Studies	64
3.2.1	Dispersal Analysis	64
3.2 2	Parametric Studies for optimal Depth of Burial (Lower Limit)	70
3.2.3	Parametric studies for Optimal Depth of Burial (Upper Limit)	77
3.2.4	Parametric Study for Thermal Radiation	85
3.3	Pressure - Time History	94
3.4	Analysis	99
3.4.1	Load Modeling of the Modules	99
3.4 2	Design Parameters	99
3 4.3	Finite Element Modeling	102
3.4.4	Static Analysis	106
3.4.5	Dynamic Analysis	110
3.5	Design of Concrete Shells	113
3.5.1	Design	113
3.5.2	Critical Buckling Stress	113
3.5.3	Yield Criteria	115
<b>Chapter - IV</b>	<b>Conclusions</b>	<b>118</b>
4.1	Suggested Algorithm	118
4.2	Parametric Studies	118
4.3	Static and Dynamic Analysis	119
4.4	Scope for Future Study	120

Appendix 'A'	121
Appendix 'B'	123
Appendix 'C'	126
Appendix 'D'	127
Appendix 'E'	128
References	129

## List of Figures

Figure Number	Title	Page Number
Fig 1.1	Suggested Layout of National Command Complex	13
Fig 2.3 1	Mechanism of Shock Wave for Near Surface Burst	13
Fig 2.3 2 (a)	Variation of Over Pressuere With Time at a Given Location	13
Fig 2.3 2 (b)	Variation of Over Pressuere With Distance at a Given Location	13
Fig 2 3.3.1	Equivalent Triangular Pulse	18
Fig 2 3.3 2	Duration of Effective Triangular Pulse	18
Fig 2.4.1	Crater Effects	21
Fig 2.5.1	Ground Shock Phenomenology	21
Fig 2.6.2.1 (a)	Compton Scattering	26
Fig 2.6.2.1 (b)	Photoelectric Effects	26
Fig 2.6.2.1 (c)	Pair Production	26
Fig 2.6.2.2	Narrow Beam Attenuation	30
Fig 2.6.2.3	Broad Beam Attenuation	30
Fig 2.10.2.1	Shallow Buried Structures	43
Fig 2.10.3.1	Soil Arching as a Function of Depth of Burial	45
Fig 2 10 5.1 (a)	Interface Stress on roof ( $DOB \leq 0.2L$ )	49
Fig 2.10.5.1 (b)	Interface Stress on roof ( $DOB > 0.2L$ )	49
Fig 2.10.5.2	Approximate Load for Estimating Vertical Rigid Body Motion of a Typical shell	51
Fig 2.10.5.3	Simplified Loading of Buried Arches and Cylinders	53
Fig 3.3 1	Proposed Algorithm	65

Fig 3.2.1.1	Expected Value (R) and Coefficient of Variation ( $\delta R$ ) of weapon Strike Distance for Nearby Aim Point	68
Fig 3 2.1.2	Probability of Failure vs Area of Facility	71
Fig 3.2 2.1	Variation of Pressure with DOB	73
Fig 3 2.2.2	Range vs Optimal Pressure for Various HOBs	75
Fig 3 2 2 3	Range vs Optimal DOB for Various HOBs	75
Fig 3 2 2 4	Total Over Pressure vs DOB	76
Fig 3 2 3 1	$\gamma$ Radiation Analysis	79
Fig 3.2.3.2	Radiation vs DOB for Different Ranges	83
Fig 3 2.3 3	Radiation vs DOB for Various Thicknesses of Concrete	83
Fig 3.3.3.4	Range vs Optimal DOB for Various HOBs	84
Fig 3.3.3.4	Range vs Optimal DOB for Various Thicknesses of Concrete	84
Fig 3.2.4.1	Thermal Radiation Analysis	87
Fig 3 2.4 2	Scaled Time for Thermal Pulse	89
Fig 3.2.4.3	Transmittance	89
Fig 3.2.4.4	Temperature vs time at Ground Surface	92
fig 3.2.4.5	Temperature vs Time for Various Depths	92
Fig 3.2.4.6	Maximum Temperature vs DOB	93
Fig 3.3.1	Surface - pressure Time History	98
Fig 3.3 2 (a)	Vertical Pressure Time History at Various DOBs	98
Fig 3.3 2 (a)	Horizontal Pressure Time History at Various DOBs	98
Fig 3.4.1	Outline Diagram of the principal Module	100
Fig 3.4.1 (a)	Load Modeling for Static Analysis	101
Fig 3.4.1 (b)	Load Modeling for Dynamic Analysis	101
Fig 3.4 3.1	Elemental and Global Coordinates	104

Fig 3 4.3 2	Finite Element Modeling of the Principal Module	105
Fig 3.4 3.3	Stress on Arbitrary Element vs Number of Elements	107
Fig 3 4 3.3	Bending Moment on Arbitrary Element vs Number of Elements	107
Fig 3 4.3 5	Maximum Stress vs Number of Elements	108
Fig 3 4 3.6	Maximum Bending Moment vs Number of Elements	108
Fig 3 4 3.7	Processor Time vs No of Elements	108
Fig 3 5 3.1	Yield Criteria for Shell Elements	117

## List of Tables

Table Number	Title	Page Number
Table 1 1	Suggested Facilities of National Command Complex	7
Table 2 2.1	Relative degrees of weapon Effects for Various Burst Conditions	11
Table 3 4 2 1	Design Parameter for a Specific Case	102
Table 3.3 4 1 (a)	Results of Static Analysis (Stresses)	109
Table 3.3.4.1 (b)	Results of Static Analysis (Deflections)	110
Table 3.4.5.1	Natural Frequencies of the Module for Various Stiffnesses	111
Table 3.4 5.2 (a)	Results of Dynamic Analysis (Stresses)	112
Table 3.4.5.2 (b)	Results of Dynamic Analysis (Deflections)	112

## SYMBOLS

$A_f$	Area of the facility
$A_{cl}$	Area of Complex
$A_h$	Average Projected Area of Human Being
$B(x)$	Buildup Factor
$C$	Compression Wave Velocity of the Concrete
$CEP_e$	Circular Error Probability in Locating the Attacker's Aim Point
$CEP_r$	Circular Error Probability of the Warhead Delivery with Respect to a known Aim Point
$C_L$	Compression Wave Velocity of the Soil
$C_o$	Ambient Sound Speed
$D$	Thickness of the Roof
$DOB$	Depth of Burial
$erfc$	Error Function
$E$	Modulus of Elasticity of Concrete
$E_{tot}$	Fraction of Total Energy in the Form of Thermal Energy
$f_{perm}$	Permissible Buckling Stress in Cylindrical Shell
$F(t)$	Force at any Time $t$
$F_{cr}$	Critical Stress
$F_e$	Cube Strength
$I$	Photon Intensity
$J$	Energy Radiated per unit Area
$k$	Air Absorption Coefficient
$K_o$	Coefficient of Earth Pressure
$L$	Span of the Structure
$L_r$	Radius Defined by the Attacker for its Successful Mission

$M_x$ , $M_y$ and $M_{xy}$	Bending Moments in shells
$N$	Number of Delivery
$P(e)$	Probability of Explosion
$P_o$	Ambient Pressure
$P_{ovr}$	Soil Over Burden Pressure
$P_{perm}$	Permissible Stress in Spherical Shell
$P_q$	Stress Applied at the Top of the Structure
$P_s$	Peak Over Pressure
$P_{so}$	Ground Surface Over Pressure
$Q$	Total Thermal Energy Received at any Distance $D$
$QF$	Quality Factor
$R$	Weapon Strike Distance
$S_o$	Strength of the Weapon Source
$t_{max}$	Maximum Time for Thermal Pulse
$T$	Transmittance
$T_x$ , $T_y$ and $T_{xy}$	Membrane Stresses in shells
$U$	Shock Front Velocity
$v(t)$	Velocity of the Structure
$w$	Deflection along $Z$ axis
$W$	Weapon Yield
$W_h$	Average Weight of Human Being
$x$	Thickness of the Shield
$Y_L$	Lower Yield Value
$Y_U$	Upper yield Value
$\alpha$	Thermal Diffusivity of the Soil
$\epsilon$	Emissivity of the Soil
$\phi$	Particle Flux Density
$\mu$	Linear Attenuation Coefficient

$\nu$	Poisson's Ratio
$\rho$	Density of Soil
$\sigma$	Stefan Boltzman Constant
$\sigma_b(t)$	Stress Acting on the Base at any time t
$\sigma_{ff}(t)$	Incident Stress Wave
$\sigma_r(t)$	Stress Acting on the Roof at any time t
$\sigma_s(t)$	Stress Acting on the Side at any time t

## ABSTRACT

The planning, layout and design of **National Command Complex** to resist all the nuclear weapon effects, to safeguard our political and military leaders in event of nuclear war has been illustrated

An attempt has been made to combat the adverse effects of weapon by using Reinforced Cement Concrete as a basic construction material. The soil cover on top of the complex is used to mitigate the radiation effects.

An algorithm to design such a specialized specialised structure been suggested. A concealed and dispersed layout of the complex has been chosen to reduce the chances of success of the attacker's mission.

The parametric studies have been performed to obtain the optimal depth of burial from blast, nuclear and thermal radiation considerations for various ranges of explosion.

Static and dynamic analysis have been performed for one of the principal module of the complex using Structural Analysis Program - IV. The results are compared and a design force has been suggested.

Finally, the module has been designed using Indian Standard Codes of Practice and checked for buckling stresses and critical moments

## CHAPTER - I

### INTRODUCTION

#### 1.1 General

Throughout the history man has sought to protect himself from hostile forces of his environment. Apart from providing shelter from natural danger he has also striven to provide shelters from military threats. Seen historically, the need for defence and improvements in the means of defence were responses to threats and to counter-improvements in the method of attack.

#### 1.2 Philosophy of Warfare

From the earliest times, strongholds were solely defensives to resist attack by primitive weapons with no great range. The defenders needed an impregnable fortress, in which to shelter. The sophistication grew in response to increased numbers of deliveries from attackers, but the basic balance between attackers and defenders remained until it was upset by Romans' development of 'siege warfare'. To counter this came construction of protective shelter inside the besieged area and the erection of tall shelters encircling walls. Thus the balance was maintained and see-saw battle continued until the end of nineteenth century.

The growth in power and sophistication of explosives and fire arms changed the earlier philosophy during World War-I, in

favour of the attacker. The defensive counter-measures merely increased the mass and strength of the structure in response to the more powerful attacks. The conflict until this time mainly confined to armed forces, who suffered twenty times more casualties than civilians. The next major shift was due to advancement in aerial warfare widely used in World War II. The civil populace behind the front line could for the first time be directly involved in the conflict. This led to further improvement in defence by development of public and private air raid shelters, which could withstand a local explosion and in some cases, even a direct hit.

### 1.3 Nuclear Environment

The development of nuclear bomb and its first use at Hiroshima (15 kT) and three days later at Nagasaki (20 kT) radically altered the threat posed by the attacker. The amount of nuclear weapon energy is so high that even if military targets are selected, the whimsically named collateral damage would result in an effect little different from that of such purely civilian targets as cities are chosen.

Parallel to this, came the remarkable improvement in accuracy of the delivery system of these devastating weapons, which is measured in terms of Circular Error Probabilities (CEPs). In fact some of the latest delivery systems have CEPs even less than a hundred meters.

#### 1.4 Protective Shelters

Thus in society an individual has only opportunity to safeguard an ordered civilization in long term, and that is by pressing the establishment of total disarmament. The removal of fear of annihilation so that no nation has enough armament to attack any neighbor nation anywhere, must be the objective. Yet there are many powerful voices around the world, who still believe, 'If you desire peace then be prepared for war'. This is dangerous nonsense when the weapons of war are not swords but nuclear warheads and it is a disastrous misconception to believe that by increasing the total uncertainty one increases one's own certainty of survival.

Thus the only defence response made possible by these developments is to seek shelter in the immediate area to protect against the harmful effect of the weapons. These shelters can broadly be divided into three categories from structural and utility point of view. These are

- i) protective shelters for civilian population.
- ii) upgraded structures for industries
- iii) specialized structures (eg Hospitals, Water supply systems, Government buildings, Command complexes )

As the national security and chances of winning a

nuclear war are completely dependent on the continuity of the chain of the command at the highest level, this present study is focused on planning, design and construction of a Command Complex at the national level to safeguard our military and political leaders in the event of a nuclear war. But the parametric studies and analysis of the present work are applicable for any hardened concrete structure to resist the nuclear weapon effects.

### 1.5 Scope of the Present Study

The scope of the present study is mainly to plan, analyze and design the 'National Command Complex'. A hardened concrete structure to mitigate the collateral nuclear weapon effects to the level tolerable to the housed operation/material/personnel is considered. To elaborate more, this protection entails

- i) nuclear blast and shock resistant design,
- ii) protection against radiation for specific period,
- iii) protection against thermal effects, and
- iv) shielding against other effects such as electromagnetic pulse (EMP), dust, debris, fires etc.

The aim of the present work is outlined as follows

- i) Construction of data charts for peak over pressure for various ranges, height of bursts and magnitude of explosion from available analytical expressions
- ii) Establish pressure time histories for various possible cases of explosions.
- iii) Threat perception and Reliability analysis for dispersal of facilities.
- iv) Parametric study to obtain optimal depth of burial for various ranges, height of bursts and magnitude of explosion, taking soil arching effects into consideration
- v) Radiation analysis for various thickness, grade and type of concrete.
- vi) Study of attenuation of radiation with depth of burial for optimum depth taking buildup factor into consideration.
- vii) Thermal Radiation Effect and its parametric study with depth of burial.
- viii) Static analysis of the principal shell module of concrete for most expected threat by using finite element method.
- ix) Dynamic analysis (Time History Analysis) of

the modules using Structural Analysis Programm-IV (SAP-IV).

- x) Design of the modules by Indian Standard Codes of practice

## 1.7 General Standard Qualitative Requirements

Some of the suggested qualitative requirements for such a complex are .

- i) Capable of housing approximately two hundred persons;
- ii) Uninterrupted operation for a minimum of thirty days;
- iii) Alternate passages for facilities;
- iv) Sufficient dispersal and alternate emergency facilities;
- v) Concealed structure;
- vi) Emergency entry and exit doors, and
- vii) Internal and external communication

## 1.8 Planning and Layout

Based on the requirements listed in the foregoing and keeping in view the functional aspects, the proposed outline plan of the complex is as shown in Figure (Fig) 1.1. It caters for the

facilities as shown in Table 1.1

**Table 1.1      Suggested facilities of National Command Complex**

S.No	Name of the facility	Qty
1	Living/Offices Rooms	12
2	Administrative facility	2
3	Power Plant	2
4	Air Filtration Unit	2
5	Hospital	2
6	Cremation Place	1
7	Fire Fighting Unit	1
8	Water Tanks	2
9	Decontamination Stations	2
10	Security Rooms	2
11	Chemical Toilets	6
12	Central Hall	1
13	Communication centers	2
14	Meteorological Station	1
15	Air Suction Unit	2

Apart from these the complex will also have passages to connect all the facilities for the movement of personnel and a jeep size vehicle.

Although the dimensions of these facilities may vary depending upon the actual functional requirements, for the purpose of this thesis, these have been kept at realistical values.

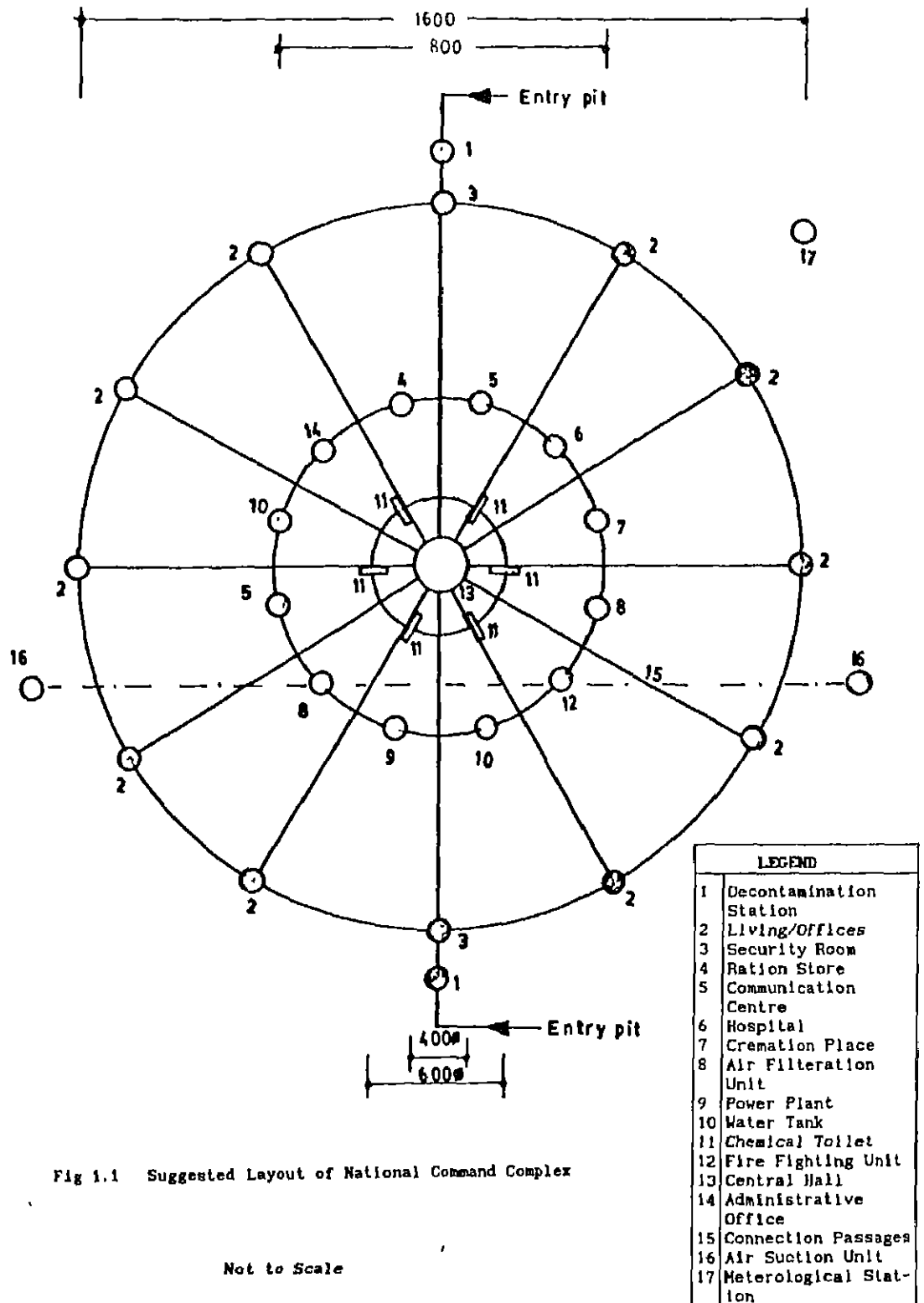


Fig 1.1 Suggested Layout of National Command Complex

Not to Scale

All dimensions are in meters

## 1.9 Organisation of the Thesis

The present work has been organised into four chapters Chapter-I covers the planning and layout aspect of the complex keeping in view the qualitative and quantitative requirements.

In Chapter-II the available literature on the subject matter has been reviewed in detail The aspects such as crater effects, ground motions and neutron radiation which are not considered in the present study have also been reviewed for the sake of completeness.

Chapter-III deals with various parameteric studies performed from optimal dispersal, depth of burial and temperature considerations The latter part of the chapter contains analysis and design of one of the principal modules of the complex The results have been discussed at the end of the each section to facilitate better understanding.

Chapter-IV concludes the present work with qualitative recommendations and future the scope of study for civil engineers in this challenging field .

## CHAPTER - II

### REVIEW OF LITERATURE

#### 2.1 Scope

The literature review for the thesis has been classified as follows

- i) Blast and Shock effects of nuclear explosion
- ii) Crater effects.
- iii) Ground motions
- iv) Nuclear radiation effects
- v) Thermal radiation effects
- vi) Other effects (eg EMP, dust, debris and fires)
- vii) Threat perception and reliability analysis for optimal dispersal of facilities.
- viii) Soil arching relations and attenuation of over pressure with depth of burial
- ix) Finite Element modeling for shell structures
- x) Static and Dynamic Analysis
- xi) Design of concrete shell structures

#### 2.2 General

The nuclear weapon effects for protective construction vary with location and the magnitude of explosion. They can be

classified as air, surface or underground burst. This location based classification is due to the variation in the quantum of the effects. A burst above 10m height is regarded as an air burst and the burst taking place below 5m is regarded as an underground burst [1]. The relative effects due to various burst condition is shown in Table 2.2.1 [2]. It is evident that the near surface burst causes maximum damage in terms of blast and radiation. It is more likely to be resorted by the attacker in the event of nuclear war. Hence, the analysis and design presented in next few chapters caters for this worst possible condition.

**Table 2.2.1 Relative Degrees of Weapon Effects for Various Burst Conditions [2]**

Burst Condition	Thermal Radiation		Initial Nuclear Radiation	Ground Shock	Air Blast	Early Fallout
	Light	Heat				
High Alt.	****	**	*		*	
Air Burst	***	****	****	*	****	
Ground	**	***	***	**	***	****
Water	***	***	***	**	***	****
Confined subsurface				****		

### 2.3 Blast and Shock Effects

When a nuclear weapon is detonated in the air, hydrodynamic expansion of bomb debris and radiation heated air produce a strong shock wave expanding in the surrounding air. Its interaction with ground surface affects the geometry and

characteristic of this expanding blast wave [1].

A surface or near-surface burst produces a hemispherical shock front that reflects from the ground. The reflected signal, travelling faster than the incident shock in the heated air, eventually takes over the incident shock and forms a Mach stem that connects the ground with the triple intersection of incident, reflected and Mach stem shock to form, producing double peak phenomenon. This can be explained as shown in Fig. 2 3.1. The incident wave (1) from a burst point above the ground is reflected in a regular reflection (2) until the angle it makes with the ground plane becomes large enough to allow the reflected wave to takeover and coalesce with the incident wave forming a Mach reflection (3). As the Mach stem grows, the contact surface (4), separating air that has experienced only the Mach shock from air that has been through both the incident and reflected shocks trails behind and connects the triple point (5) with the surface. However, air flow above the contact surface does not completely turn parallel to the surface by the reflected shock and retains some downward momentum. This results in eventual compression at the surface (6) as the downward moving double shocked air above the contact surface is stopped. This compression (7) distorts and chews up the tail of the contact surface stream line (6) and rises the pressure. The Mach shock itself represents a lower pressure than that behind the reflected wave in the regular reflection region, but the second shock quickly builds to appreciably higher values at the transition. The important aspects of this phenomenon as shown in Fig.2 3.2 (a) and (b) are as follows [1]

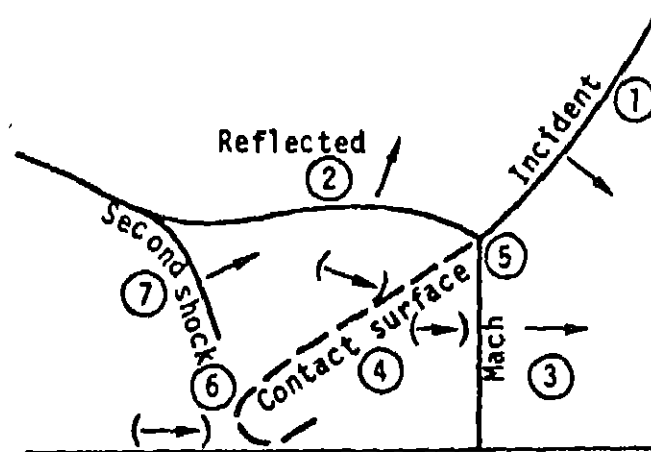


Fig 2.3.1 Mechanism of Shock Wave for Near Surface Burst

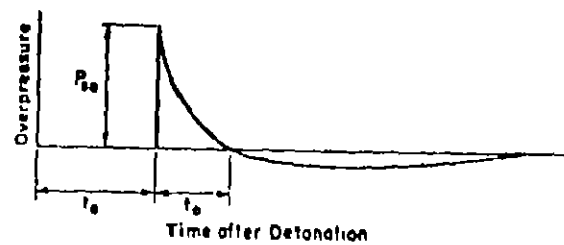


Fig 2.3.2 (a) Variation of Over Pressure with Time at a given location

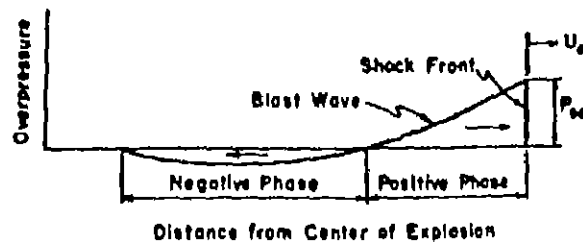


Fig 2.3.2 (b) Variation of Over Pressure with distance at a given location

- i) Time of arrival
- ii) Peak pressure
- iii) Positive phase duration
- iv) Pressure - Time History

### 2.3.1 Over Pressure and Dynamic Pressure

The transient pressure which is greater than the atmospheric pressure is defined as the over pressure. The peak over pressure is the maximum value of the over pressure at a given location. As the blast wave arrives at a given point, the over pressure rapidly increases from zero to the peak pressure. The magnitude of this peak over pressure and its variation depends on the location and the magnitude of the explosion.

As the blast wave moves outward from the explosion, the flow of the mass of air behind the blast front produces a wind. The resulting pressure is termed as dynamic pressure which is a function of density of air and the wind velocity behind the shock front. The speed of the shock front  $U$ , is given by [1,3 and 4]

$$U = C_o \left[ 1 + \frac{6 P_s}{7 P_o} \right] \quad (2.3.1.1)$$

where,

Assuming that air is an ideal gas

$\gamma$  = Specific heat ratio = 1.4

$C_o$  = Ambient sound speed

$P_o$  = Ambient pressure

$$P_s = \text{Peak over pressure}$$

This approximation is correct within  $\pm 8\%$  for the peak over pressure less than 700 MPa [1]

A finite time is elapsed between the detonation and the arrival of the blast front at a given location. This time of arrival is dependent primarily upon the weapon yield and distance from the point of burst.

The duration of the blast wave is characterized by two distinct phases, viz positive and negative phases. During the positive phase the over pressure rises very rapidly from ambient to peak value and then subsides more slowly to ambient pressure once again. For some height of burst in the mach reflection region, a second peak pressure increase may occur, which may be higher or lower than the first pulse. As the distance from the explosion increases the positive phase of the dynamic pressure becomes somewhat longer than that of peak over pressure. In the second phase a partial vacuum is created, then the wind blows towards the point of detonation. This phase is comparatively longer than positive phase and the peak rarely exceeds 28 kPa below the ambient value. Although smaller in magnitude it is important for design of blast doors and latches [1].

### Yield Scaling

The air blast parameters are normally given in terms of 1 kt or 1 Mt. These parameters can be determined for other

yields of interest by scaling from the reference values [1]

These scaling laws [1] are

$$\begin{aligned}\frac{R}{R_1} &= \left( \frac{W}{W_1} \right)^{1/3} \\ \frac{t}{t_1} &= \left( \frac{W}{W_1} \right)^{1/3} \\ \frac{I}{I_1} &= \left( \frac{W}{W_1} \right)^{1/3}\end{aligned} \quad . \quad . \quad (2.3 \ 1 \ 2)$$

where

$R_1$	Range at which pressure of interest occurs
$W_1$	Reference yield
$R$	Actual range
$W$	Actual yield
$t_1$	Reference time
$t$	Actual timeand
$I_1$	Reference impulse

### 2.3.2 Pressure - Time Histories

Analytical expressions and several graphical methods are available [1 ,2 and 3] to find the over pressures and the time histories. These were developed and used since 1962 after the Nevada test sites results. But the detailed experiments conducted in 1970's have provided a better definition of the region of the double peaks, an important area in the early mach reflection region at high over pressures. These highly nonlinear analytical expressions to calculate the peak over pressures and corresponding

time history are given in Appendices 'A' and 'B'. These expressions use the scaled ground range and height of burst and thus yield results corresponding to one kT. Hence the different times and ranges must be scaled to the actual yield of requirements.

### 2.3.3 Approximate Analysis for Time Histories

If computers are not available to solve these expressions then the time histories can be approximated by triangular equivalents, having the same initial peak-over pressures but different time depending upon the expected time of structural response. These equivalent triangular pulses are as shown in Fig 2.3.3.1. The durations are determined from the Fig 2.3.3.2. Reference [1] provides the procedural details for approximate analysis.

### 2.3.4 Dynamic Pressure

In many a case the, drag forces associated with the strong transient wind behind the shock front are mainly responsible for actual damage, specially in the case of above ground structures. Some of the structures are described as drag sensitive, as they are quickly enveloped by the blast wave and thus the primary translatory forces are due to the results of the drag forces. These forces are the function of the size, shape and

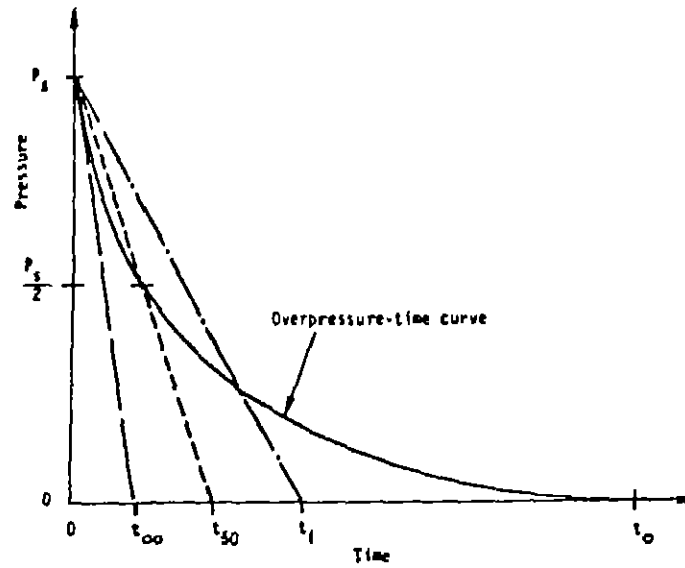


Fig 2.3.3.1 Equivalent Triangular Pulse

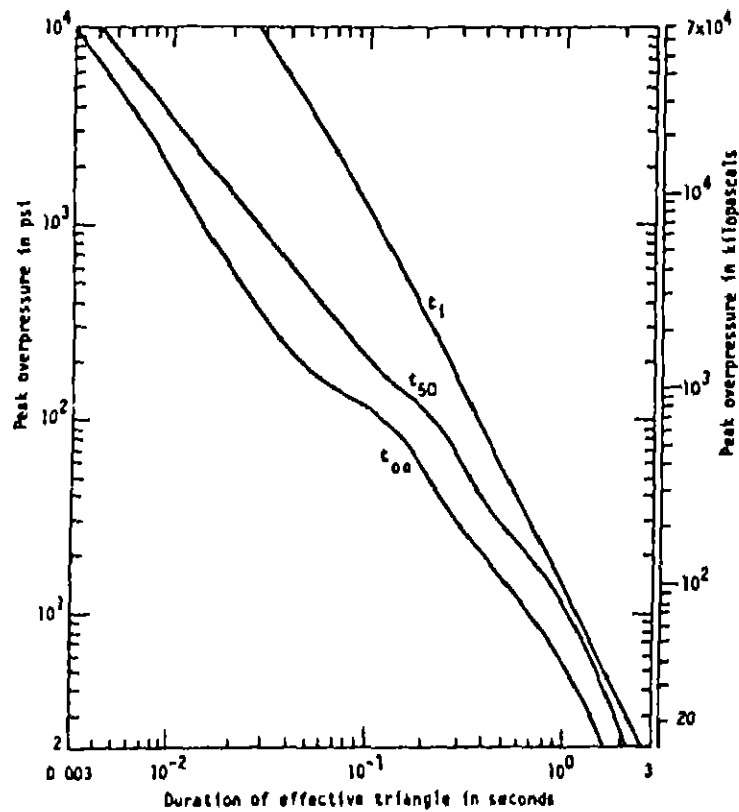


Fig 2.3.3.2 Duration of Effective Triangular Pulse

transient dynamic pressure

The analytical expressions for peak dynamic pressure dynamic pressure time histories, time of arrival, duration and impulse are given in References [1 and 3]. As it is always advantageous to bury the structure for many obvious reasons hence the dynamic pressure is not of much importance in the present context. However, this aspect is very important for the above ground structures and should be taken care while designing such structures. The references [1,2] give details of this aspect for the design of nuclear structures.

#### 2.4 Crater Effects Due to Nuclear Blast

This phenomenon occurs when there is very near, surface or under ground burst. The approximate dimensions and other terminology associated with this aspect are as shown in Fig 2.4.1.

The dimensions are predicted from two tests conducted at Nevada test site, before nuclear test ban treaty, one in alluvial soil and other in hard rock. For other conditions these can be interpolated. The scaling laws exist here to standardize for 1 kT explosion. For the other yields crater dimensions can be predicted by applying a yield scaling exponent.

The height of burst (HOB) or depth of burst (DOB) is measured from the original ground surface to the centre of weapon release. The most significant to catering is the low air burst, when HOB less than  $3 \text{ m/kT}^{1/3}$ .

The volume of crater from air burst in various

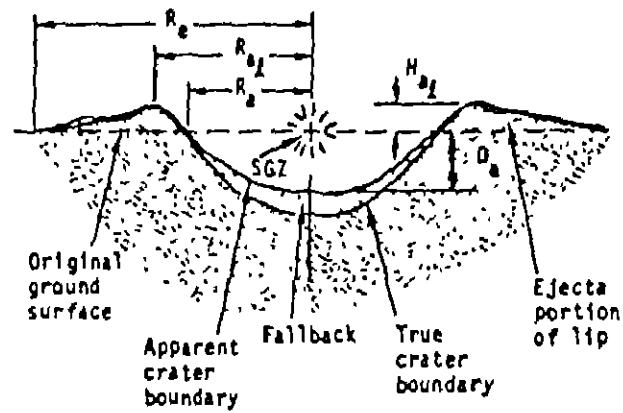
homogeneous geologies are given in literature [1] and can be estimated approximately

## 2.5 Ground Motions

Another important phenomenon occurring due to blast in very near surface burst or ground burst is the induced ground motion as shown in Fig 2 5.1 Here the air blast loading is shown in super seismic condition i.e. the velocity of the air blast shock is greater than the propagation velocity of the peak compressive stress in upper material. The initial ground shock is a response to the air blast loading immediately above the point of interest. The ground shock component associated with the local air blast is said to be air slap induced.

As the air blast shock front slows, the velocity becomes less than the propagation velocity of the peak compressive stress in the upper material. The initial ground shock response at this time is caused by the air blast upstream from the point of interest. Situations where the ground motions are outrunning the blast are of importance from the analysis considerations [1].

The ground shock is divided in two components, the air slap induced and upstream induced components. The wave forms for each are superimposed temporally to arrive at the composite wave form. The ground shock from all sources other than local air blast is considered upstream ground induced shock, including shock from directly coupled energy and upstream air blast. This is further divided into *body wave* and *surface wave components*, because at



LEGEND:

- $D_a$  = Apparent crater depth
- $H_{a1}$  = Height of apparent lip
- $R_a$  = Apparent crater radius
- $R_{a1}$  = Crater radius to apparent lip
- $R_e$  = Ejecta radius
- SGZ = Surface ground zero

Fig 2.4.1 Crater Effect

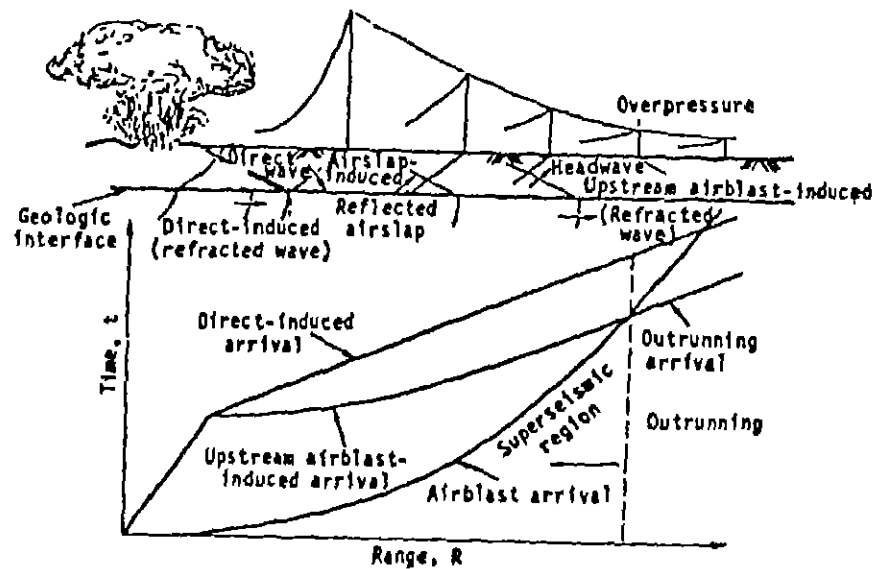


Fig 2.5.1 Ground Shock Phenomenology

longer range the upstream induced motions are primarily associated with surface wave [1]

To gain maximum advantage from the nuclear explosion on the strategical targets, the weapon is detonated in the air. Hence it very unlikely to expect any surface burst from the attacker. Therefore this effect has not been considered for the design and analysis in the present context

## 2.6 Radiation Effects

One of the special features of the nuclear explosion is that it is associated by emissions of the nuclear radiations, which is one of the governing criteria for design of such important structures [5]. These radiations can be categorized as

- i)  $\alpha$  particles
- ii)  $\beta$  particles
- iii)  $\gamma$  radiation
- iv) Neutron radiations

### 2.6.1 $\alpha$ and $\beta$ Radiations

The ranges and penetration power of these two radiations are very limited they cannot reach the surface of the earth from air burst even when the fireball touches the ground. Hence the initial radiation consists of mainly  $\gamma$  rays and neutron radiation within a minute of the explosion [2].

Both of these radiations produce harmful effects on living organism as shown in Appendix (Apex) 'C'. It is this highly injurious nature of these radiations combined with their long ranges that make them such a significant aspect of nuclear radiation. The energy associated with this is approximately three percent of the total energy release [1]

#### 2.6.2 $\gamma$ - Rays

As it is evident that the  $\gamma$  rays being the most important aspect of the nuclear radiation as far as the shielding is concerned. This has been reviewed in greater detail under the following parameters.

##### a) Sources

In nuclear explosion the  $\gamma$  rays are generated due to the fission process. They are also generated by the neutron produced in the fission process. When these neutrons are captured by non fissionable nuclei material they get converted into compound nucleus which is of very high energy state. The excessive energy may be liberated as  $\gamma$  radiation called captured  $\gamma$  radiation. Here the interaction of neutron with nitrogen nuclei is of importance because  $\gamma$  rays produced thereby is of very high energy and attenuates very little with distance. The  $\gamma$  rays are also produced due to inelastic scattering. As the fission fragments are highly radioactive in nature they also generate an appreciable

amount of the radiation in the very first minute of the explosion  
This radiation is known as *delayed gamma radiation* [2]

### b) Technical Aspect of $\gamma$ radiation

Rigorous analysis of the radiation calculation due to  $\gamma$  rays needs the knowledge of interaction of the  $\gamma$  rays with matter, as a result of which photons are scattered or absorbed. These interactions can be classified as follows [5]

- i) Compton effect
- ii) Photoelectric effect
- iii) Pair Production

#### Compton effect

The total extent of Compton scattering per atom of material with which the radiation interacts is proportional to the number of electrons in the atom i.e. to the atomic number for all materials, irrespective of their atomic weight. The effect is shown in Fig 2.6 2 1.(a) [5].

#### Photoelectric effect

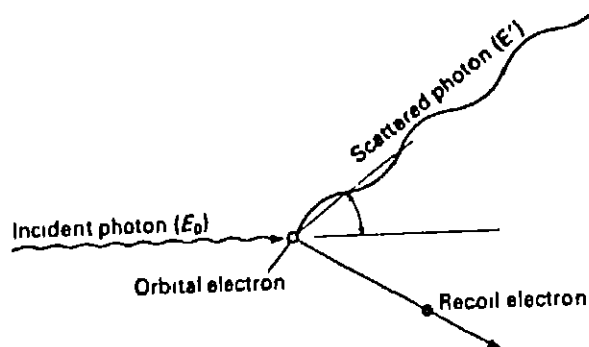
It is an interactive process in which an orbital electron is ejected from an atom by a photon. This occurs when the photon possesses a higher energy than the binding energy of the

orbital electron with which it collides. All the energy of the incident photon in excess of the electron binding energy is transformed into kinetic energy of the ejected photo-electron. As the binding energy of the orbital electron increases the photoelectric effects decrease rapidly as inversely proportional to the cube of energy. The photoelectric effect is proportional to the fifth power of the atomic number and the microscopic cross section is proportional to  $(N Z^5 E^{-3.5})$ . The other forms of radiation may also arise but they can be disregarded for practical purposes. The phenomenology is sketched as shown in Fig 2.6.2 1 (b) [5].

#### Pair Production

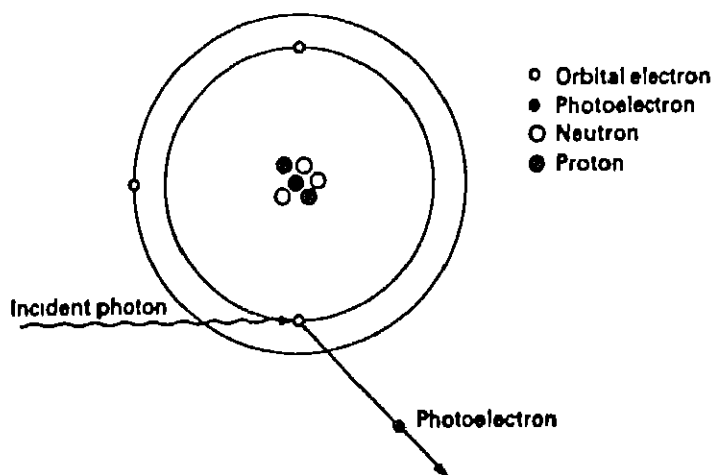
The process in which a photon is converted into a pair of electron, positron and negatron, in the coulomb field of an atomic nucleus is called pair production. The incident photon is replaced by a positron-negatron pair. All the energy is absorbed. As the rest mass of an electron is equivalent to 0.51 Mev. Thus to have the kind of pair production incident photon should not have energy less than 1.02 Mev. The balance of the photon energy then appears as kinetic energy (KE) of the electron-positron pair.

The probability of pair production is more when the atomic number  $Z$  of the absorber is high. The cross section can be approximated to  $Z^2$ . The cross section also increases with the photon energy, and at high energies it becomes the dominant interaction process of photons with matter (Fig.2.6.2 1 (c)).

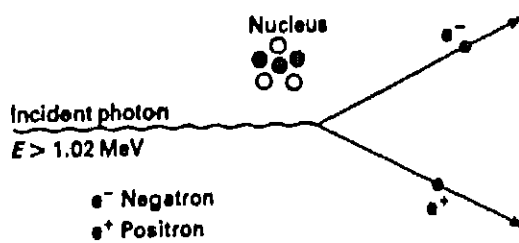


$E = \text{energy}$

(a) Compton Scattering



(b) Photoelectric Effect



(c) Pair Production

Fig 2.6.2.1.

Hence it can be concluded that interaction of photon increases with the increase of atomic number of the material through which the  $\gamma$  ray passes. Each interaction does completely absorbs or reduces the energy of incident photon. Hence it can be said that material containing the elements of high atomic weight will be more effective as  $\gamma$  ray shield. Also with energy greater than 1.02 Mev the absorption is minimum. This process of the interaction is shown in Fig 2.6.2.1 (c) [5 and 6]

### c) Photon Attenuation

Consider a slab of absorber material placed between a narrow collimated source of mono magnetic photons and a narrow collimated detector as shown in Fig 2.6.2.2. The arrangements are such that the scattered radiation from striking the detector and any interaction of photons with the absorber material are prevented leading to complete removal of photon from the beam.

Then, in a thickness  $dx$  of the absorber the fractional reduction in the photon intensity  $I$  is given as  $-dI/I$ , which is related to the narrow beam attenuation  $\mu$  and the thickness  $dx$  by the following relation

$$dI/I = -\mu dx \quad (2.6.2.1)$$

If the initial photon intensity is  $I_0$  and the thickness of the absorber is  $x$  then

$$\int_{I_0}^{I_X} \frac{-dI}{I} = \mu \int dx \quad (2.6.2.2)$$

and

$$I = I_0 e^{-\mu x} \quad (2.6.2.3)$$

These equations are referred as exponential absorption equations

The linear absorption coefficients are dependent on the density of the material. The density often does not have a unique value but is dependent on the physical state of the material. Thus to obviate the effects of variations the linear absorption coefficient for reference purposes is expressed as mass attenuation coefficient ( $\mu/\rho$ ) [5 and 6].

#### d) Photon Absorption

The energy absorption coefficient are related with the loss or absorption of energy as a result of photon interaction with matter, whereas the attenuation coefficients concern the number of photons which are affected. Thus the amount of energy absorbed determines the effect of radiation. Similar to the attenuation coefficients the values of the absorption coefficients are available in references [7]

### e) Broad Beam Attenuation and Buildup Factors

The above mentioned equations are only applicable to cases in which the scattered compton interaction may be regarded as essentially removed from the  $\gamma$  ray beam. It reasonably holds good for narrow beams or for the shields of narrow thicknesses but fails for broad beams or thick shields, which is the case in nuclear explosion. The allowance of multiple scattering is made by the provision of a '*buildup factor*' as shown in Fig 2 6.2.3. Hence these equations can be modified as [5]

$$I = I_0 B(x) e^{-\mu x} \quad (2.6.2.4)$$

where

$B(x)$             Buildup factor

The *buildup factor* depends on many factors such as energy of the photon source, angle of incidence, nature, thickness of the shield and the type of detector response. The values of the *buildup factors* for various ranges of energy and shield material is given in references [7]. However, some of the relevant ones for the purposes for the thesis are given in Apex 'D'

### f) Transmission of $\gamma$ ray and Source Geometry

A point source is regarded as a volume of the source material the dimensions of which are small in comparison with the distance between the source and the position of the detector. If a point source emits particles in all the directions isotropically, the radiation is assumed to be evenly distributed

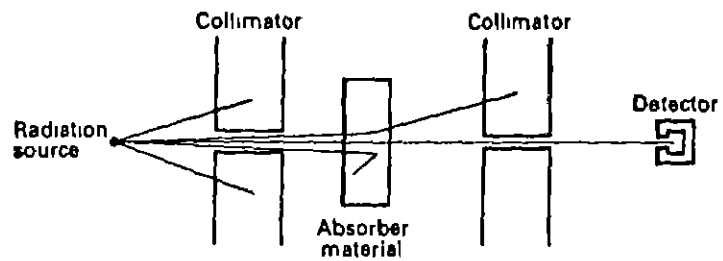


Fig 2.6.2.2 Narrow Beam Attenuation

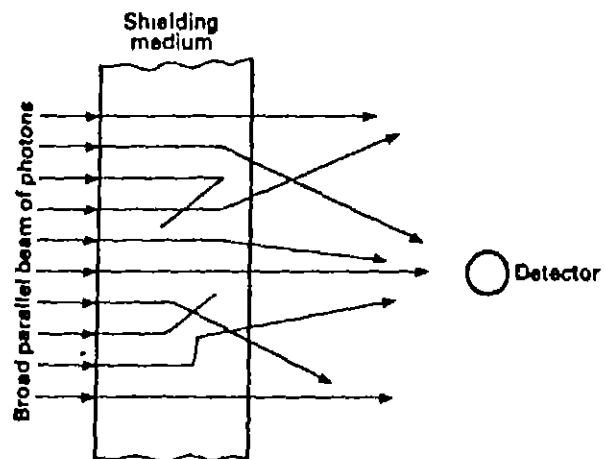


Fig 2.6.2.3 Broad Beam Attenuation

over the surface of a sphere whose area is  $4\pi x^2$ , where  $x$  is the distance between the source and detector. The flux at a distance  $x$  is given by [2 and 5]

$$\phi = \frac{S_o}{4 \pi x^2} \quad (2.6.2.5)$$

where

$$\begin{aligned} \phi &= \text{The particle flux} \\ S_o &= \text{Strength of the source} \end{aligned}$$

If it is considered that the point source is surrounded by a spherical shield then the flux density at a distance  $x$  from the source is

$$\phi = \frac{S_o}{4 \pi x^2} e^{-\mu t} \quad (2.6.2.6)$$

where

$$t \quad \text{Thickness of the shield}$$

#### g) $\gamma$ Ray Spectrum

The information concerning the energy spectrum of the initial radiation is important because of the susceptibility of the living organism under various energy spectra. The attenuation properties of the air, shielding material and the response of the

detector instrument is dependent on the energy distribution of the  $\gamma$ -rays. Although the exact spectrum at some distance from the source is difficult to obtain but with the knowledge of initial  $\gamma$  radiation spectrum at the source and existing data on scattering and absorption of different energy in the intervening medium can be employed to provide the spectrum at a given distance. Reference [2] provides relevant information on this important aspect of the nuclear explosion.

### 2.6.3 Neutron Radiation

As in the case of the photons, which interacts with the electrons in atoms, the interaction of the neutrons with electrons is negligible. They interact rather with the nuclei of the atoms, and their interaction is very much dependent on the KE of the neutrons.

#### a) Nuclear Reactions

Nuclear reaction generally be expressed by the following type of the equations [5]



where

X	Target nucleus
Y	Resulting nucleus

- a            The bombarding particle  
b            Emitted particle

In the transmission of the neutron through matter many types of reactions or interactions are possible. In the shielding calculations for neutrons the reactions which are significant are [3] elastic, inelastic and neutron capture.

#### b) Effective Removal Cross Section

Most neutrons which penetrate thick shields are fast neutrons, having energy greater than 7 Mev. The effective removal cross sections are the cross sections which may be used in exponential absorption equation to obtain valid results concerning the attenuation of fast neutrons [5]. Hence,

$$I = I_o e^{-\sum R_x} \quad (2.6.3.2)$$

Where

- $\sum R_x$     Effective macroscopic removal cross  
          section for material  
 $I_o$         Initial fast neutron intensity  
 $I$          Emergent fast neutron intensity

But, if the sufficient number of hydrogen atoms are not in the shield then the intensity of the emergent neutron may be higher than the calculated from equation 2.6 3 2 [5]

Similar to the photons the energy spectrum for the neutrons from explosion of nuclear bombs are available in the literatures [2] The calculation for the integrated neutron flux can also be done in similar fashion

For greater effects in terms of radiation special Neutron Bombs are available with most of the developed countries but they do not generate significant amount of shock effects The most part of the energy of these weapons are consumed to liberate radiation particles producing very little shock effects Since, the shock effects are the principal criteria for design of such structures, the effects of neutron radiation due to fission bombs in calculations can be neglected without much loss of accuracy [5]

## 2.7 Thermal Radiation

Thermal radiation is rarely a driver in the design of a hardened structure. By making provisions for protection against sterner threats of nuclear blast and nuclear radiations the designer almost automatically protects the structure against thermal radiation threat. However, it is pertinent to evaluate the thermal effects to the internal environment of the facilities. Also the study of thermal effects are important for the structural engineer to incorporate the temperature effects in the analysis

and for the selection of appropriate material accordingly. The approximate radiant exposures for ignition of various materials for low air bursts are given in literature [1 and 2].

## 2.7 1 Technical Aspect of Thermal Radiation

Although spectroscopic studies made in course of weapon tests revealed that it does not behave exactly like a black body, the assumption of a black body behavior for the fireball, however serves as reasonable approximation in interpreting the thermal radiation emission characteristics. For a black body the distribution of radiant energy over the spectrum can be related to the surface temperature by Plank's equation [2 and 8] as

$$E_{\lambda} = \frac{8 \pi h c}{\lambda^5} \cdot \frac{1}{e^{h c / \lambda k T} - 1} \quad (2.7.1)$$

where

$E$	Energy of the black body
$c$	Velocity of the light
$h$	Plank quantum action
$T$	Absolute temperature
$hc/\lambda$	The energy of the the photon wavelength.

The rate of emission of energy  $J_{\lambda}$  can be given for a black body for a given wavelength[2 and 8]

$$J_{\lambda} = \frac{c}{4} E \quad (2.7.2)$$

where

$$J_{\lambda} \quad \text{Energy per unit area}$$

According to Stefan Boltzman law the total amount of energy  $J$  radiated per unit area per second is given by

$$J = \sigma T^4 \quad (2.7.3)$$

where

$$\begin{aligned} \sigma & \quad \text{Stefan Boltzman constant} \\ & = 2 \pi^5 k^4 / 15 h^3 c^2 \\ & = 5.67 \text{ E-5 erg/cm}^2 \cdot \text{s} \end{aligned}$$

Next important parameter to be considered is the total thermal energy received at some distance  $D$  from the point of explosion which can be given by the law of physics [2] as

$$Q = \frac{E_{\text{tot}}}{4 \pi D^2} \cdot e^{-kD} \quad (2.7.4)$$

where

$k$	Absorption coefficient of the air
$E_{tot}$	The fraction of the total weapon energy available as effective thermal radiation
$Q$	Total energy received at distance $D$

it is also important to know the total duration of the effective pulse for the calculation of the incident energy at any distance on the earth surface. Although no theoretical formulas are available for this time pulse time calculation, the tests conducted at the Nevada test site before nuclear test ban treaty provide some guidelines to evaluate this pulse time. The graphs are available for various energies of the explosion in literature [2].

The attenuation of the thermal energy by a transient source in any medium is a complex function of the conduction and radiation phenomenon. It depends on the thermal properties of that medium and can be evaluated for the buried structure. Reference [9 and 10] provides the fundamental approach in this aspect of thermal radiation.

## 2.8 Other Effects

The other important effects of nuclear weapons which could be of importance to a design engineer are as follows

### i) Electromagnetic Pulse Effects

- ii) Debris
- iii) Dust and
- iv) Fires

#### 2.8.1 Electromagnetic Pulse Effects

The nuclear explosion releases large amount of energy. Approximately one percent of it get converted in EMP. The nature of the pulse depends on the type, magnitude, range and the height of explosion. Its effect on any system depends on the physical and mechanical characteristics and the location of the system. These effects are more relevant to electronic equipments which are to be housed inside the complex. Special care should be taken for installation of these equipments [1 and 2]

#### 2.8.2 Debris

Debris is any material that can be carried along by the blast from a nuclear explosion. Such a material can cause casualties and damage to the facilities as a result of high energy impact or accumulation, or both. This effect may cause severe damage to above ground and mounded structures. But due to many obvious reasons these command complexes are either shallow or deep buried, where the effects of debris are none. Hence this effect has not been discussed in great detail. However, literature provides adequate information to combat this threat [1].

### 2 8.3 Dust

The dust is produced due to the following two reasons

- 1) Propagation of the blast wave from the point of explosion
- 11) Thermal energy produced due to the blast

This phenomenon is again pertinent to above ground and mounded structures and therefore has not been reviewed keeping in view of the present requirements [1]

### 2.8.4 Fires

Although shallow buried structures have very little probability of catching fires, But civil engineers should avoid use of fire prone materials in construction of such complexes. References [1 and 2] give details of the threshold energy of various materials of civil engineer's concern [1 and 2].

## 2.9 Threat Perception and Reliability Analysis

The threat perception and accordingly reliability analysis depends on various strategical and classified military informations. If the information on the attacker's objective and defender's actual requirements are available then this can be performed for actual scenario. In the present

context, due to absence of the actual information this has been performed only for dispersal of the facilities by assuming fictitious capability of the attacker. However some of the guidelines available in Reference [1] can be summarised as follows

- i) Develop demand scenario
- ii) Identify the failure modes and criteria
- iii) Calculate demand applied in each mode
- iv) Construct series and parallel network of failure mode probabilities
- v) Allocate goal to each failure mode
- vi) Calculate for each failure mode, capacity required to satisfy allocated share the goal
- vii) Identify worst case mean capacity for each failure mode and,
- viii) Write, for each failure mode, deterministic design specification for identified worst case mean capacity

## 2.10 Blast Loading and Soil Arching Effects

The choice of siting the complex is basically a compromise between the strategical and technical requirements. The complex can be above ground, mounded or buried. The type and the quantum of the force subjected on the structure for each of these choices are totally different. Therefore the approach for

analysis is different for each of these choices. The loading on the structures for below ground structures have been described in next few sections

#### 2.10.1 Air Blast Loading on Below Ground Structures

The below ground structures can be categorized as shallow or deep buried depending on the depth of the burial (DOB). This division is relative and depends on the span of the structure. The classification is as given below [1 and 11].

- i) Shallow buried      (  $0.2L \leq DOB \leq 1.5 L$  )
- ii) Deep buried      (  $DOB > 1.5 L$  )

where

L      Span of the structure

The design of deep buried structures is primarily governed by the soil overburden pressure. The blast has very little effect on the structure. These structures have other peculiar problem associated with them. They are generally not economical and hence not preferred unless warranted. Therefore as a part of literature review these structures have not been considered.

The shallow buried structures experience partially the blast load due to soil arching and at the same time they are also

influenced by the soil overburden. The total effects are different at different depths. Hence for ease of the analysis these can further be classified as [1]

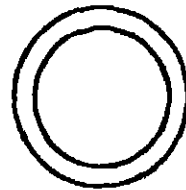
- i) Shallow Buried
- ii) Surface Flushand,
- iii) Mounded Structures

### 2.10.2 Shallow Buried Structures

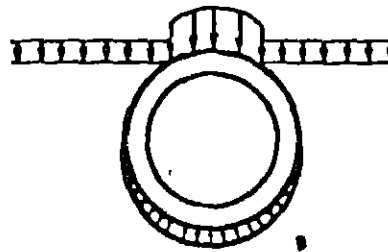
The shallow buried structures have a DOB over the roof or crown, such that  $0.2 L \leq DOB \leq 2.0 L$ , where  $L$  is the clear span between the supporting walls of a roof slab or the horizontal diameter of an arch or cylindrical structure. The structures located at  $0 \leq DOB \leq 0.2 L$  are treated as surface flush. The loads produced by the nuclear explosion on the structure buried in a medium with finite shear strength are influenced not only by structure/medium interaction as the loaded structure deforms but also by the effects of propagating transient stress wave [1]. A typical shallow buried structure is as shown in Fig 2.10.2.1.

### 2.10.3 Soil Arching

It is defined as the ability of the soil to transfer the loads from one location to the another in response to a relative displacement between the locations. Thus it is solely dependent



(a) BURIED HORIZONTAL CYLINDER



(b) VERTICAL STRESS COMPONENTS ON HORIZONTAL CYLINDER  
SHORTLY AFTER ARRIVAL OF THE INCIDENT WAVE

Fig 2.10.2.1 Shallow Buried Structure

on the properties of the soil. This can effectively redistribute the loads on a roof slab away from the flexible center of span to hard support points such as columns and structural walls. This has also been practically verified for buried arch structures. The effect of soil arching is to force a high mode compression failure. For very hard structures the soil arch may not form because the shear capacity of the soil may have exceeded, and no redistribution would have occurred. Various analytical expressions are available to incorporate these effects [1, 12, 13 and 14]. But the most generalized equation based on a differential approach that produces realistic results is given in Reference [1] and rewritten as

$$\frac{P_q}{P_{so}} = \exp \left[ \frac{-2 K_o (\tan \phi) (a + 1) b L^2}{a L^2} \right]$$

.. (2.10.3 1)

where

- $P_q$  Stress applied at the top of the structure ,
- $P_{so}$  Ground surface over pressure
- $K_o$  Coefficient of earth pressure at rest
- $\phi$  Angle of internal friction for soil
- $L$  Span length of the structure
- $a$  Factor relating length of a structure to its span length
- $b$  Factor relating depth of burial to its span length

Fig 2.10 3.1 shows soil arching as a function of depth of burial.

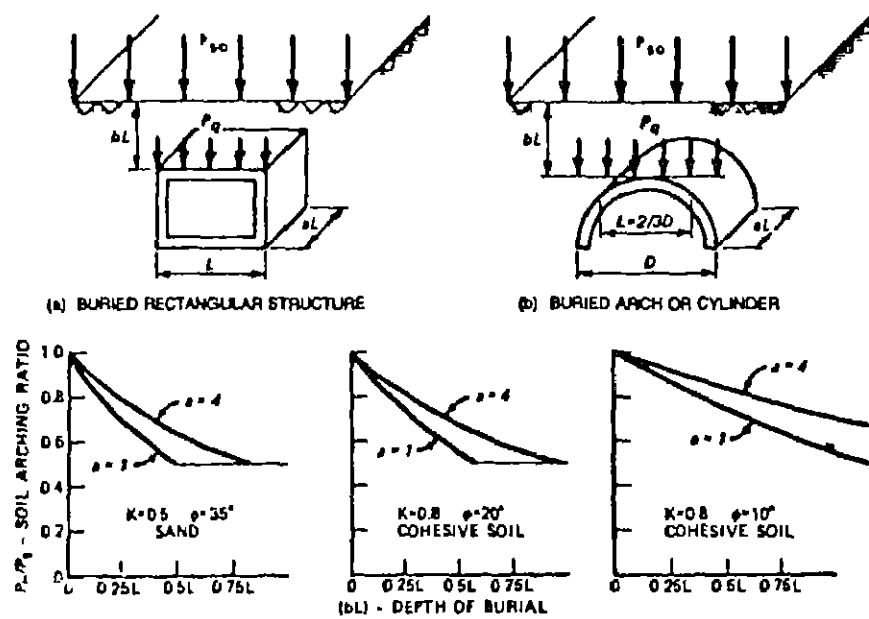


Fig 2.10.3.1 Soil Arching as a Function of Depth of Burial



# D Thickness of the roof surface

The time  $t$  can be taken as zero at the time incident wave strikes the roof surface. Also for high yield weapons it is reasonable to assume the incident pressure as ground surface pressure but for low yield weapons less than 50kT it is recommended to take soil arching into consideration. Thus the equations can be rewritten as

$$\sigma_r(t) = \sigma_{ff}(t) \left( 2 - t/t_d \right) \quad \text{for } t \leq t_d$$

$$\sigma_r(t) = C_a \sigma_{ff}(t) \quad \text{for } t > t_d$$

(2.10 4.2)

where

$C_a$  Soil arching ratio

The stress acting at the base of the structure is given by

$$\sigma_b(t) = \rho C_L v(t) \quad \text{.. (2 10.4 3)}$$

where

$\rho$  Density of the soil

$C_L$  Compression wave velocity of the soil

$v(t)$  Velocity of the structure.

An acceptable approximation to the stresses acting at the base can be given by

$$\sigma_b(t) = \sigma_{ff}(t) \quad (2.10.4.4)$$

The stresses acting at the side of the structure can be given by

$$\sigma_s(t) = K_o \sigma_{ff}(t) \quad (2.10.4.5)$$

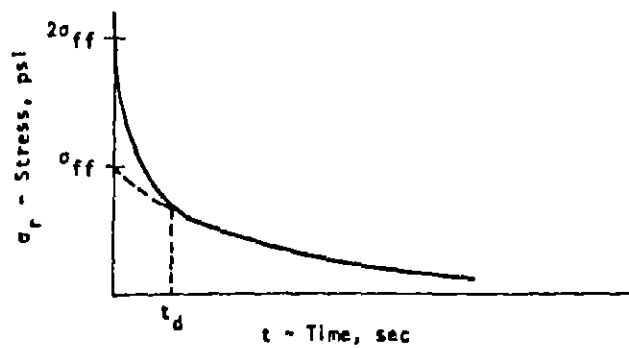
where

$K_o$             Coefficient of the lateral earth pressure  
at rest

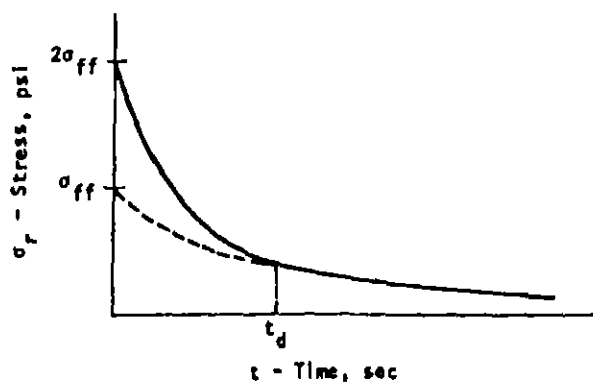
#### 2.10.5    Shallow Buried Shells

The analysis of a shell structure is complicated by its geometry [1,15]. The multidirectional effects become important at the instant the incident wave strikes the structure. The process of the interaction can be described as shown in the Figs 2.10.5.1 (a) and (b).

As the incident wave strikes the upper crown of the structure, the stress at the crown is assumed to be double and due to this, structure begins to moving down as a rigid body. Within a very short period of time the entire half portion of the shell experiences stresses due to motion of the cylinder into the soil, while the incident wave has not progressed far beyond the crown. As the incident wave propagates downwards, reflected wave continues to occur on the upper half of the cylinder because the peak reflected stress is a function of the angle between the



(a) DOB Less than  $0.2 L$



(b) DOB greater than  $0.2 L$

Fig 2.10.5.1 Interface Stress on Roof

incident wave and tangent to the cylinder at the point where the incident wave contacts the cylinder, as well as function of the velocity of the structure at the time the incident wave arrives at the point. The load modeling on the structure is shown in Fig 2.10.5.2 [1].

By idealizing the cylindrical structure as octagon the load in the vertical region A can be given by

$$F_a(t) = 0.8 \sigma_a(t) R L \quad (2.10.5.1)$$

where

$F_a(t)$  Total vertical load in the Region A

$R$  Cylinder outside radius

$\sigma_a$  Stress in the region A

The load in the region B can be given by

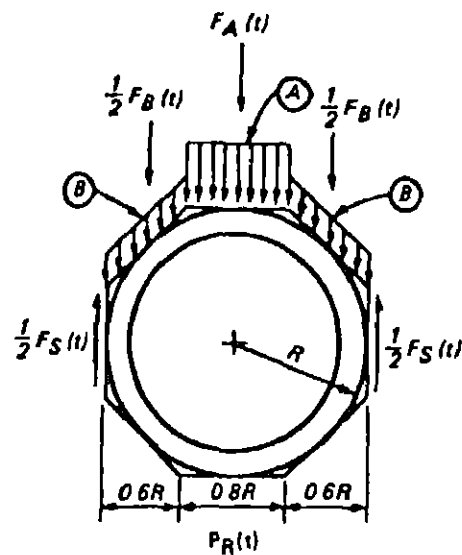
$$F_b(t) = 0 \quad \text{For } 0 \leq t < 0.3 R / C_L$$

$$F_b(t) = 1.2 \sigma_b(t) R L \quad \text{For } t \geq 0.3 R / C_L$$

... (2.10.5.2)

The total resisting incident load is taken as

$$F_r(t) = 2 \rho C_L v(t) R L \quad \dots (2.10.5.3)$$



(a) OCTAGONAL APPROXIMATION AND ACTING LOADS

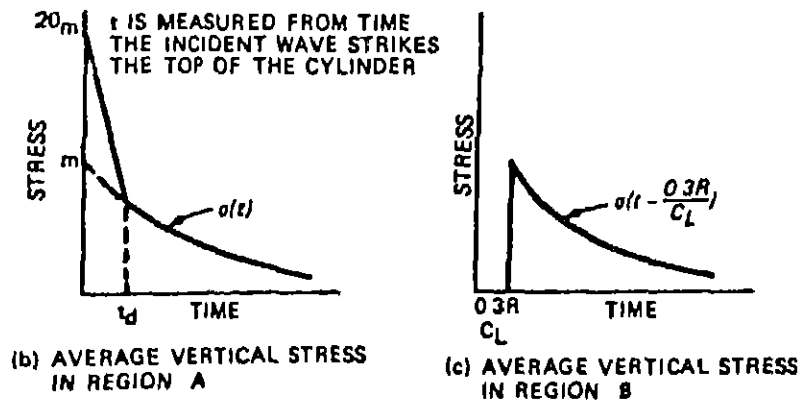


Fig 2.10.5.2 Approximate Vertical Loads for Estimating Vertical Rigid Body Motion of a Typical Shell

Hence ignoring shear the equation of motion can be given as [1]

$$M \ddot{v}(t) = F_a(t) + F_b(t) - F_r(t) \quad (2.10.5.4)$$

where

$\ddot{v}(t)$       Acceleration of the structure

$M$             Mass of the structure

Another simplified method to analyze these buried shell structures by approximating the blast force and lateral pressures is shown in Fig 2.10.5.3 [1], is suitable for use with single degree of freedom system analysis which gives reasonable results.

## 2 10.6      Mounded Structures

The loads expected on these structures are intermediate between the above and underground cases. The inclined earth boundaries reduce the drag and reflected pressure to quite an extent but even then it is very significant up to a slope of 1:4. The geometric complexity and non-uniform loading associated with mounded structures are not readily translatable into simple interaction model. However the bounding loads and motions of the mounded structures can be estimated by considering the above ground, buried or surface flush extreme. Since there are other

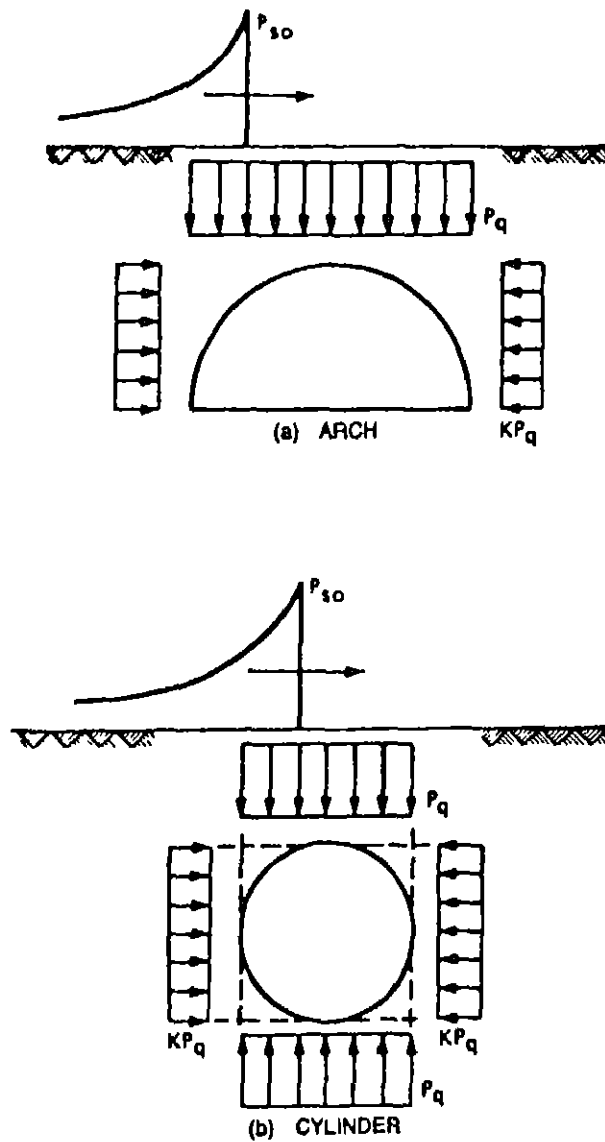


Fig 2.10.5.3 Simplified loading of Buried Arches and Cylinders

effects of explosion which are more dominant on these structures, this choice is not suitable for the complex.

#### 2.10.7 Surface Flush Structures

When the DOB is less than  $0.2L$  the structure is treated as surface flush due to its different response than shallow buried structures. The load acting on the roof of the structure can be analyzed as follows [1]

$$\sigma_r(t) = \sigma_{ff}(t) \left( 2 - t / t_d' \right) \quad \text{For } t \leq t_d'$$

$$\sigma_r(t) = \sigma_{ff}(t) \quad \text{For } t > t_d'$$

.(2.10 7.1)

where

$\sigma_r(t)$                       Stress acting on the roof at any time  $t$

$t_d'$                        $Z_s / C_L$  or  $12 D / C$  whichever is smaller

$Z_s$                       Depth of the structure roof  $\leq 0.2L$

As far as pressures at side and base of the structures are concerned they can be taken same as in case of the shallow buried ones.

## 2.11 Analysis and Design

The analysis of shell structures can be performed either as thin or thick shells [16 and 17]. The thin shell analysis does not take into account the stresses and moments in the direction along the thickness of the shell assuming it to be of a very small quantity. The thin shell analysis approach can be adopted in the present context without much loss of accuracy in the results. As the structure and loading are symmetric about one axis

The membrane stresses and bending moments can be calculated by the following general shell equations [17]

$$T_x = \frac{\partial^2 F}{\partial Y^2} \quad (2.11.1)$$

$$T_y = \frac{\partial^2 F}{\partial X^2} \quad (2.11.2)$$

$$T_{xy} = \frac{\partial^2 F}{\partial X \partial Y} \quad (2.11.3)$$

$$M_x = D \left( \frac{\partial^2 w}{\partial Y^2} + \nu \frac{\partial^2 w}{\partial X^2} \right) \quad (2.11.4)$$

$$M_y = D \left( \nu \frac{\partial^2 w}{\partial X^2} + \frac{\partial^2 w}{\partial Y^2} \right) \quad (2.11.5)$$

$$M_{xy} = -D \left( 1 - \nu \right) \frac{\partial^2 w}{\partial X \partial Y} \quad (2.11.6)$$

where

$F$  Stress function which gives the in plane

stress when the bending is also considered

$w$	Deflection along $z$ - axis
$D$	Flexural rigidity $= \frac{E d^2}{1 - \nu^2}$ and
$\nu$	Poisson's ratio

The analysis of the shells can be performed using SAP-IV [18]. This current version of SAP-IV has facilities for static and dynamic analysis of linear structural systems. This program has proven to be a very flexible and efficient tool. This is coded in FORTRAN-IV and can easily be modified as per the requirements. The fundamental approach for static and dynamic analysis using SAP-IV are given in next sections.

### 2.11.1 Static Analysis

The static analysis performed by the SAP-IV can be summarised as follows

- i) A static analysis involves the solution of the equilibrium equations [18]

$$K U = R \quad (2.11.1.1)$$

which is followed by the calculation of element stresses

- ii) The load vector  $R$  is assembled at the same

time as the structure stiffness matrix are formed. The solution of the equation is obtained by the large capacity linear equation solver SESOL. This subroutine uses the Gauss elimination on the positive definite symmetrical system of equations. In the program, the  $L^TDL$  decomposition of  $K$  is used and hence

$$L^T v = R \quad (2.11.1.2)$$

$$v = D L u \quad (2.11.1.3)$$

where the solution for  $v$  in the equation is obtained by the reduction of the load vectors, the displacement vectors  $u$  are then calculated by back substitution [18].

iii) After the nodal point displacement has been evaluated, sequentially the element stress displacement matrices are read and the element stresses are calculated.

### 2.11.2 Dynamic Analysis

The dynamic analysis is performed to obtain the following parameters

- Free vibration frequencies
- Mode shapes

- Displacements and rotations
- Stress and bending moments

The approach of the SAP-IV for the analysis is as described in the following

- i) The mode shapes and frequencies are obtained by solution of the generalized eigenvalue problem [18]

$$K \phi = \omega^2 M \quad (2.11.2.1)$$

where

$\omega$  Free vibration frequency

$\phi$  Mode shapes

- ii) In the dynamic response analysis the solution of the equation of the equation [18]

$$M \ddot{u} + C \dot{u} + K u = R(t) \quad (2.11.2.2)$$

where

$R(t)$  Can be a vector, arbitrary time varying or effective loads resulting from ground motion.

iii) In the present context of the thesis  $R(t)$  is an arbitrary time varying load due to a nuclear blast at a given range and depth of burial. Hence the Response History Analysis by direct integration is performed using SAP IV

iv) The program uses Wilson- $\theta$  method, which is unconditionally stable.

v) The Rayleigh damping is assumed, which can easily be taken into account in the form of mass and stiffness proportion and is given by the equation

$$C = \alpha M + \beta K \quad (2.10.2.3)$$

where

$\alpha$  and  $\beta$  are mass and stiffness proportional damping coefficients.

### 2.11.3 Design

The design of structure is performed by using following Indian Standard Codes of Practices

IS:456(1978)	Plain and Reinforced Concrete[19]
IS:2210(1962)	Shell and Folded Plates[20]
IS:4991(1968)	Blast Resistant Design[21]

The check on the limiting stress is given in [22] for plates and shell elements

## 2.12 Comments on Literature Review

It is evident from the foregoing review that the literature provides sufficient guidelines and approach for designing these structures. The approach may vary depending upon the requirements of the defender. The following points are considered for design of complex

1) It has been experienced that the above ground structures are economical only for peak over pressures less than 170 kPa. But for below ground structures the depth of the burial is a factor which depends on various economical and structural load parameters, which is one of the findings of the thesis

ii) The choice of below ground structure is due to the following reasons

- It fulfills the military requirements
- It does not experience dynamic pressure which is generated due to the following wind.
- The radiation is taken care by the soil thickness which is an economical and

effective radiation shield material.

- Thermal radiation does not have significant effects on the below ground structures.

iii) Although the choice of burial reduces the impact of the nuclear forces but it presents a complicated loading due to the following

- Structures experience static soil overburden pressure in addition to the blast pressure
- The load prediction on these structures is complicated due to the soil arching effect
- The transient stress wave propagation in the medium with finite shear strength is a complex phenomenon
- The structure is subjected to active or passive earth pressure

iv) The shells are preferred because of their shape which makes the magnitude of the net loading smaller than that developed on the box shaped ones. In addition they (domes and arches) have a great vertical and lateral strength characteristics and may be of the most economical form. However added cost is needed in terms of forms.

v) The cylindrical and spherical shells and their

combinations are a better choice, as the loading is symmetric. These can be analyzed as thin shells using standard methods for membrane and bending components

vi) The finite element modeling of the modules can be done by assuming the modules on the rigid foundation. The other nodes have degrees of freedom in all the six directions. The loading may be either static peak over pressure or the time histories depending upon the choice of the analysis. The openings can be modeled by assuming different element type and material properties at those positions

vii) The thin shell analysis is performed since the shells do not have significant displacements and rotations in the direction of the thickness

viii) The membrane stresses and bending moments can be obtained using SAP-IV [18] with suitable modifications.

ix) The design of the shell structures should be performed by using IS-456(1978) by limit state method for the principal modules of the complex

x) The check for critical stress due to buckling should be performed as per IS-2210(1962) code for shell

structures

xi) The Johnsen's failure theory for concrete shells/plates has been applied in the present context for checking principal moments in the structures. The Reference [22] provides adequate details on this aspect.

## CHAPTER - III

### DESIGN AND ANALYSIS

#### 3.1 Proposed Algorithm

Taking into consideration the available technical information on the subject matter and the defence strategical requirements, an algorithm shown in Fig 3.1.1 is suggested, to design a specialized structure as command complex, subjected to multifacet forces. This suggested algorithm incorporates the various possible effects of nuclear explosions at appropriate stages. Thus a basic guideline to design such complexes of national interest is suggested.

The planning and layout of the complex in the foregoing has been done as per this algorithm.

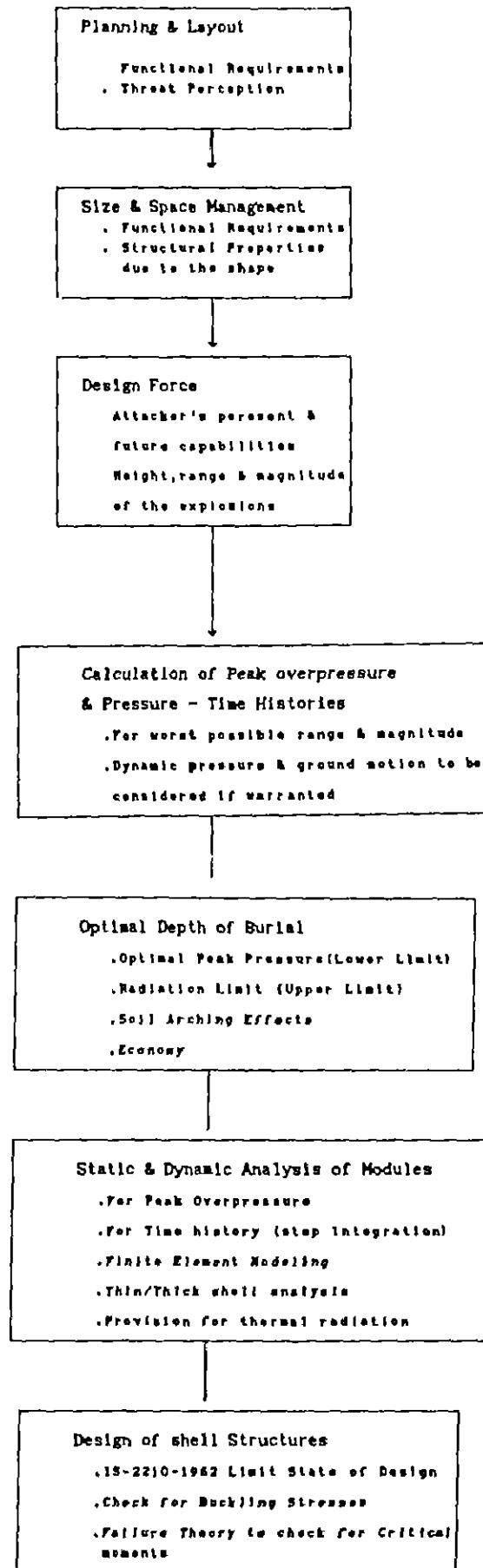
#### 3.2 Parametric Studies

Various parametric studies which are general in nature for any type of the nuclear blast resistant structures may be carried out using the foregoing algorithm stated in Fig 3.1.1.

##### 3.2.1 Dispersal Analysis

This analysis has been performed to obtain the optimal dimensions and maximum dispersal of the complex keeping in view the attacker's capabilities. The assumptions made to perform this

Figure 3.1.1 Proposed Algorithm for Design of Nuclear Blast  
Resistant Structures



analysis are given in succeeding paragraph

### Assumptions

Assuming that the attacker has capabilities to

- i) launch only one bomb at the complex
- ii) obtain the correct location if the target  
size =  $A_{cl}$
- iii) correctly aim at the target if the target  
size =  $A_{cl}$

Based on the above mentioned assumptions the problem is formulated as given below

### Formulation for Dispersal Analysis

If

the max plan area of the facility =  $A_f$  and,  
the area of the complex =  $A_{sc}$

then,

the probability of obtaining correct location for a  
target size  $A_f$

$$\begin{aligned} \text{pocl}(A_f) &= A_f / A_{cl} && \text{if } A_f < A_{cl} \\ &= 1 && \text{if } A_f \geq A_{cl}. \quad \dots (3.2.1) \end{aligned}$$

probability of correctly aiming at the target size  $A_f$

$$\begin{aligned} p_{ca}(A_f) &= A_f / A_{ci} && \text{if } A_f < A_{ci} \\ &= 1 && \text{if } A_f \geq A_{ci} \end{aligned} \quad (3.2.1.2)$$

Probability of correctly aiming the target once located

$$p_{cal}(A_f) = p_{ocl}(A_f) * p_{ca}(A_f) \dots \quad (3.2.1.3)$$

Also, if

$CEP_r$       Circular probable error of the warhead  
delivery with respect to known aim point

$CEP_e$       Circular probable error in locating the  
attacker's aim point

then

the expected value of the warhead - strike distance  $R$   
is (Fig 3.2.1.1) given by [1]

$$R = 1.064 \sqrt{CEP_r^2 + CEP_e^2} \quad (3.2.1.4)$$

and if the probability of the warhead landing in the  
radius  $L_r$

$$\begin{aligned} p(wl) &= L_r^2 / R^2 && \text{if } L_r < R \\ p(wl) &= 1 && \text{if } L_r \geq R \end{aligned} \quad (3.2.1.5)$$

where

$L_r$       is the radius defined by the attacker for  
its successful mission

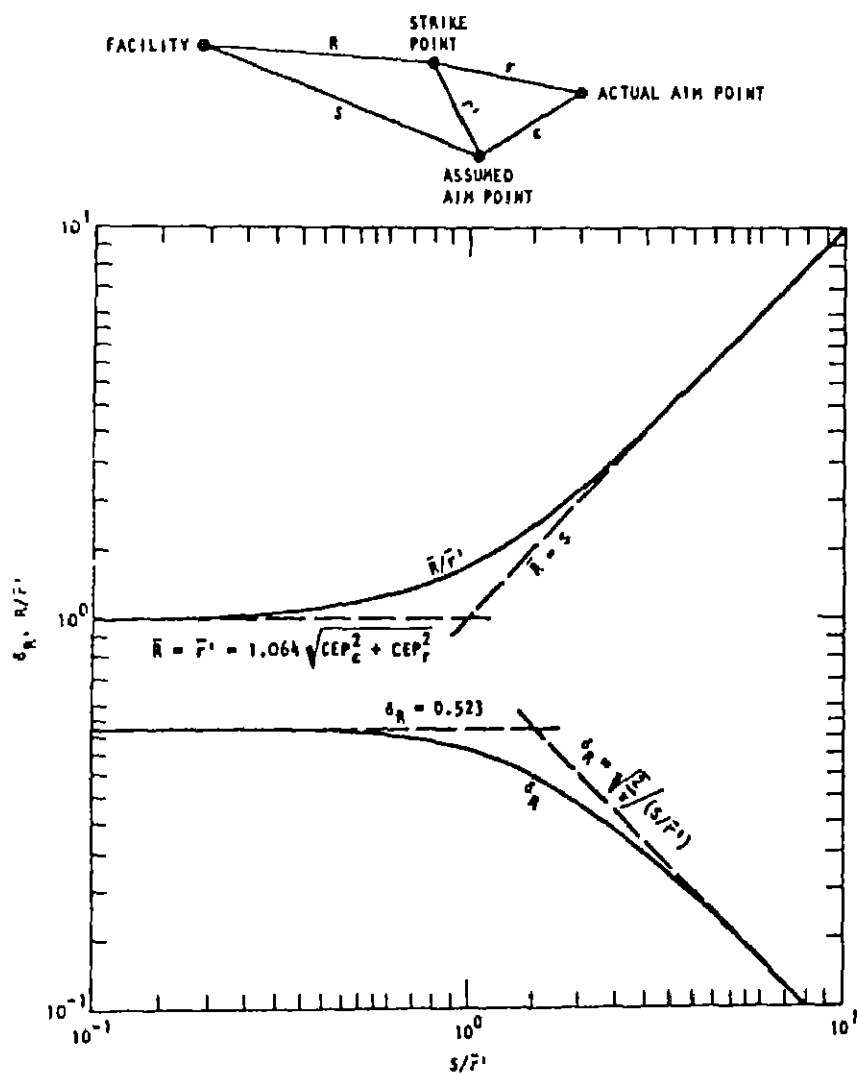


Fig 3.2.1.1 Expected Value ( $R$ ) and Coefficient of Variation ( $\delta R$ ) of Weapon Strike Distance for Nearby Aim point

If, the probability of the explosion is  $p(e)$ , then the probability of a successful mission

$$p_s(A_f) = p_{cal}(A_f) \cdot p(w1) \cdot \frac{N}{2} p(e) \quad (3.2.1.6)$$

where

$N$             number of delivery

$p(e)$         probability of the explosion of the  
warhead once launched

and the probability of failure of the attacker's mission  
can be given as

$$p_f(A_f) = 1 - p_s(A_f). \quad \dots \quad (3.2.1.7)$$

provided there is only one facility existing in the  
radius  $L_r$

It is evident from the foregoing formulation that the probability of the failure of the attacker's mission is a function of the plan area of the facility.

Hence, it is desirable to minimize the size of the facilities and disperse the same to an extent so as to reduce the probability of success of the attacker's mission. A computer routine was written to solve the equation 3.2.1.6 to perform the parametric study to correlate the size of the facility and the probability of the failure of the attacker's mission. The study is preliminary in

nature as more classified military information which is secret in nature is required for a reliable situation. However, it provides a basis to assess the reliability of such complexes.

### Results and discussion

The results plotted as shown in Fig 3.2.1.2 are based on following assumed capabilities of the attacker

CEPr	=100m
CEPe	=20m
Lr	=300m
N	=1

It is evident from the results that to have very high chances of survival the facilities should be made smaller in the size. For the facility size of 30 sq m the probability of the failure of the attacker's mission is 98% which is quite reasonable. The dispersal of the facilities should be more than the attacker's defined radius for a successful mission. Therefore the important facilities should have dispersal of approximately 300m and less important facilities may have dispersal of 150 - 200m to keep the compactness of the complex.

#### 3.2.2 Parametric studies for Optimal Depth of Burial (Lower Limit)

As it is evident that the blast pressure decreases exponentially as the DOB increases [1], whereas the overburden

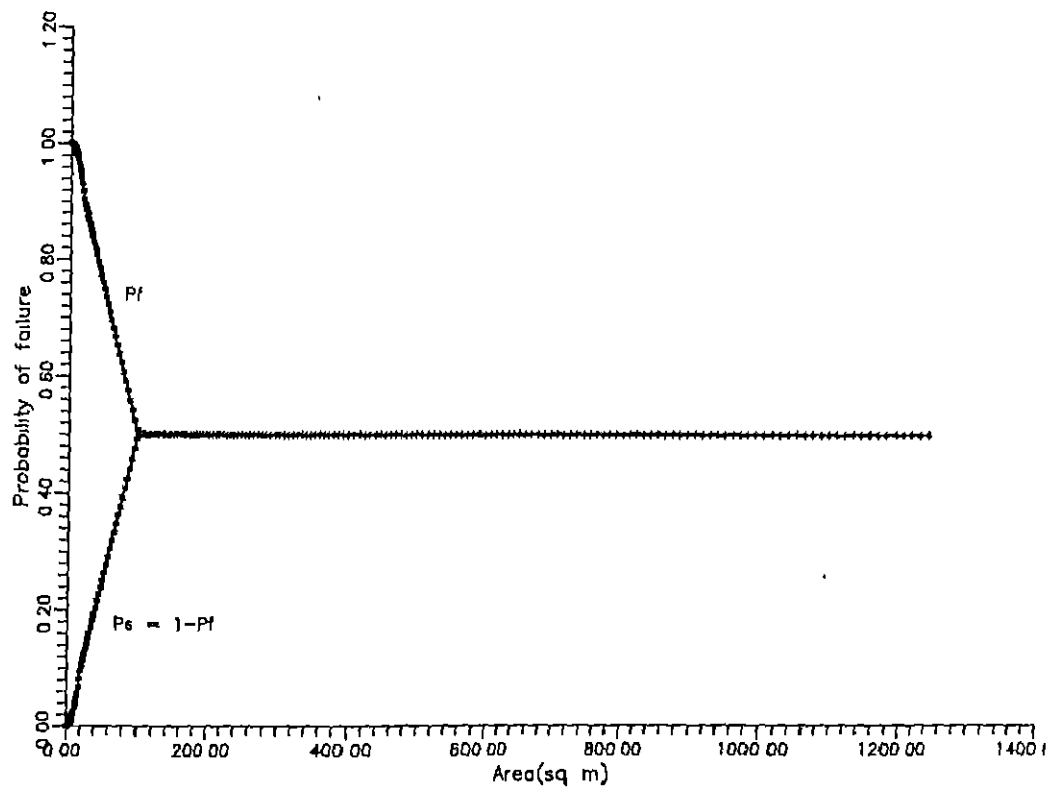


Fig 3 2 1 2 Probability of Failure vs Area of The Facility



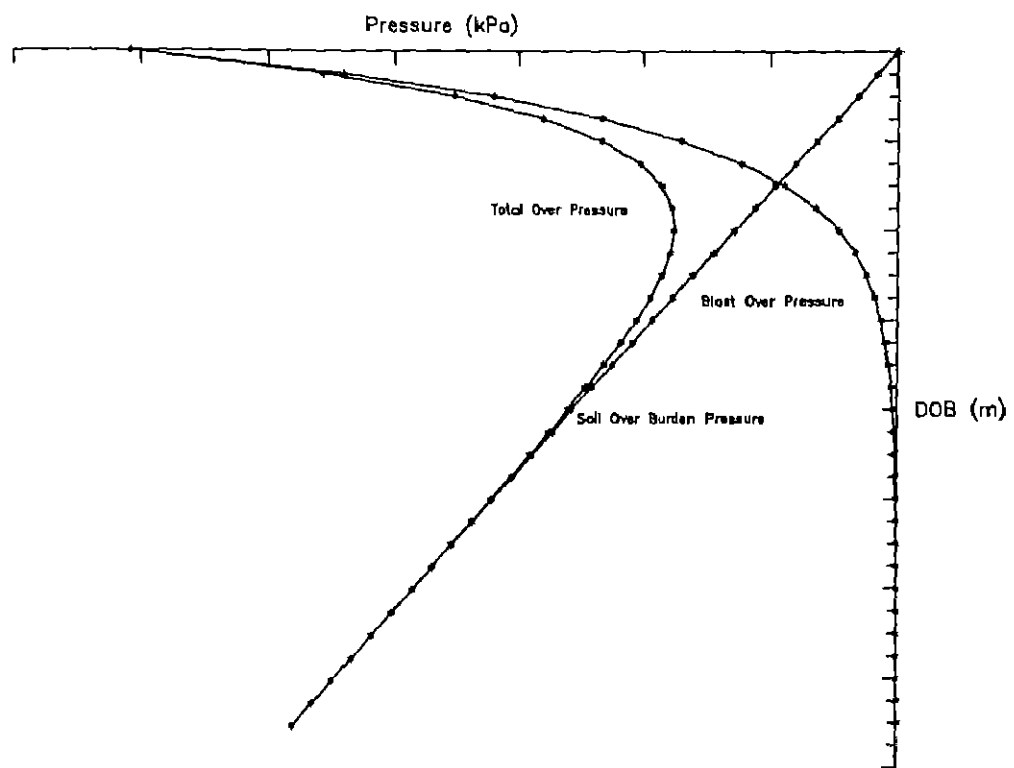


Fig 3.2.2.1 Variation of Pressure with Depth of Burial

the analytical expression as given in  
Apex 'A'

$P_q$	The attenuated over pressure at the DOB under consideration.
$K_o$	Coefficient of earth pressure at rest
$\phi$	Angle of internal friction of the soil
$a$	Factor relating length of the structure to span
$b$	Factor relating DOB to the span
$L$	Length of the structure

Hence, the total Over pressure at any depth is given as,

$$P_{total}^{(DOB)} = P_{ovr}^{(DOB)} + p_q^{(DOB)} \quad (3.2.2.3)$$

A computer program is written to solve the equation 3.2.2.3 to obtain the optimal depth of burial (for minimum total over pressure) for various ranges and heights of burst for parametric study. The following parameters have been assumed constant in the program. The values of these parameters are given as

$$\gamma = 1.6 \text{ kg/m}^3$$

$$\phi = 20^\circ$$

$$K_o = 0.8$$

$$L = 6.0\text{m}$$

$$a = 2/3 L$$

$$b = 2/3 L$$

$$\text{Magnitude of Explosion} = 20\text{kT}$$

The results of the studies have been plotted as shown in Figs 3.2.2.2, 3.2.2.3 and 3.2.2.4 for different feasible cases

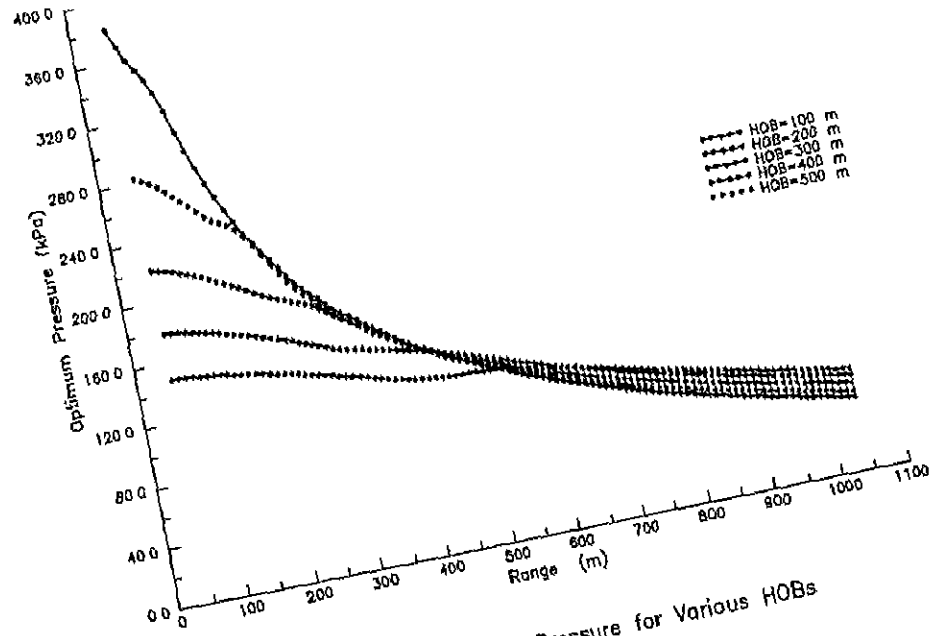


Fig 3.2.2.2 Range vs Optimal Pressure for Various HOBs

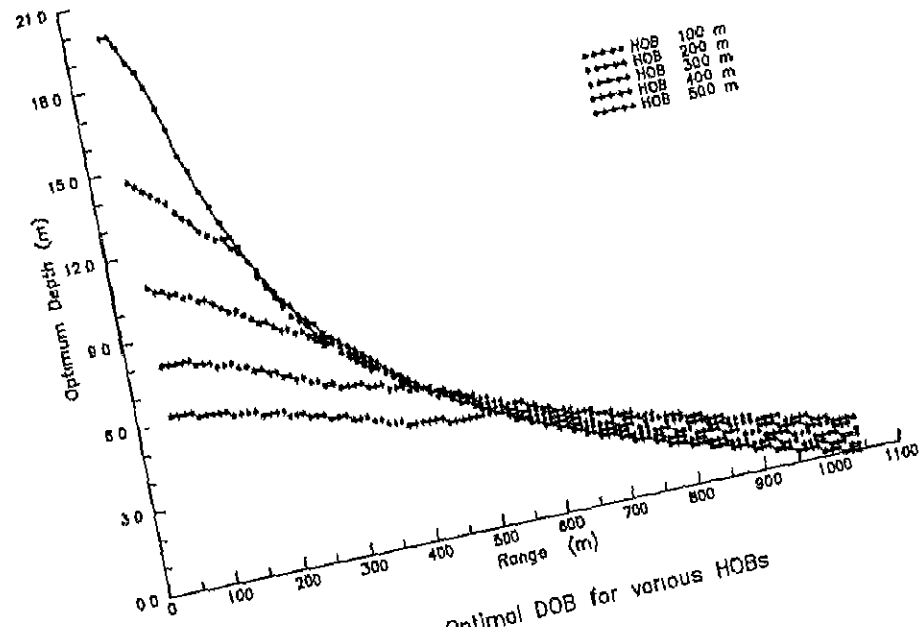


Fig 3.2.2.3 Range vs Optimal DOB for various HOBs

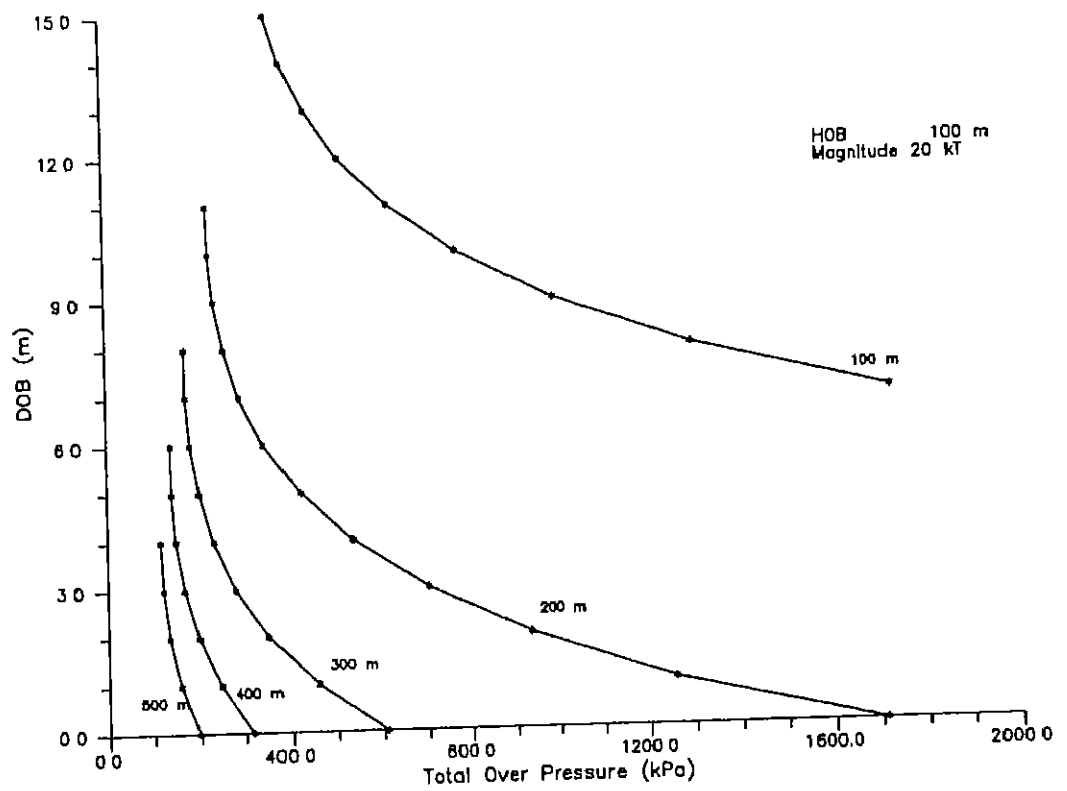


Fig 3.2.2.4 Total Over Pressure vs Depth of Burial

and are discussed in succeeding paragraph.

### Results and Discussion

The study is of general nature and provides the lower limit or (maximum) depth of the burial for shallow buried structures from total over pressure considerations

It is evident from the graphical results that for near surface bursts the values of optimal pressures and corresponding DOBs, for low ranges up to 500m are quite unstable. These ranges should be avoided for construction. For HOBs up to 500m the optimal pressure and DOBs for 500-1000m range are more or less same and presents realistic values for design. Fig 3.2.2 4 can be taken as a design chart for obtaining correct DOB and corresponding pressure for precise calculations

#### 3.2.3 Parametric studies for Optimal Depth of Burial (Upper Limit)

Another criteria for deciding the DOB for nuclear structures is radiation analysis. It is learnt from literature [1,3] that though the radiation is not a primary consideration for design but cannot be overlooked. Therefore the upper limit of DOB is governed by radiation. In the present context upper limit has been obtained by keeping  $\gamma$  - radiation limit as 0.3 rem for personnel inside the citadel.

The principal approach adopted to obtain the minimum depth of burial for various ranges, HOB and Magnitude of explosion from

radiation consideration for different thickness is of the ordinary reinforced cement concrete is explained in Fig 3.2 3 1 The formulation of the problem is in the following

#### Nuclear Fission Data

1 kT	=	$2.6 \times 10^{25}$ Mev Energy
1 Fission	=	200 Mev
1 Fission	=	7 Mev release of energy
1 rad	=	0.01 J/Kg = 100 ergs/grm
1 Mev	=	$1.6 \times 10^{-6}$ ergs

#### Assumptions

- i) Calculation of only primary and spontaneous flux is considered. It is presumed that if a person is able to sustain the initial concentrated dose, he/she would be able to survive under the reduced cumulative doses, due to residual radiation.
- ii) The personnel living inside the citadel are exposed to the worst  $\gamma$  ray flux.
- iii) For a common human being the exposure should be below 0.3 rem.
- iv) Residual radiation has not been considered as it is an extremely small quantity.
- v) The neutron radiation has been taken as half of the  $\gamma$  ray equivalent, as the fission and

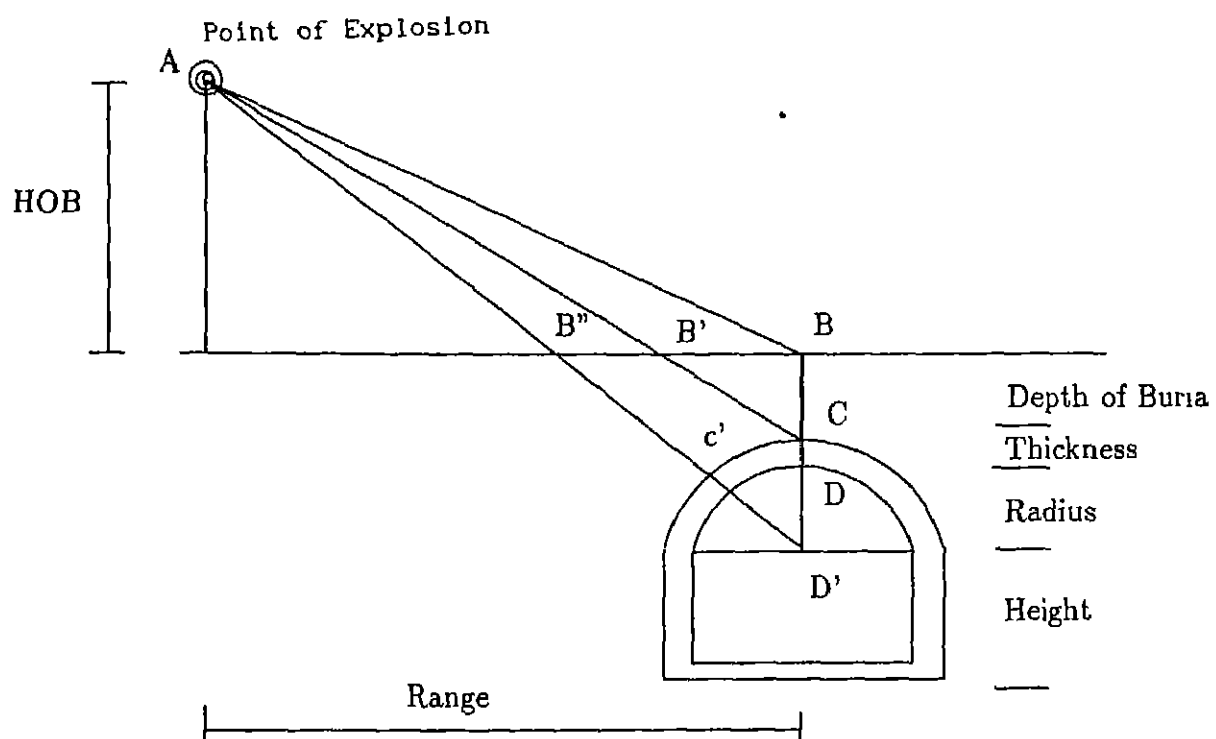


Fig 3 2.3 1 Gamma Radiation Analysis

fusion bombs do not generate neutrons as  
primary weapon effects

### Formulation

Let the flux at be A =  $\phi_A$

Then

$$\phi'_A = \frac{\phi_A}{4 \pi y^2} \quad (3.2.3.1)$$

$$\phi_B = \frac{\phi_A}{4 \pi AB^2} \quad (3.2.3.2)$$

$$\phi_C = \phi_B e^{-(\mu_a / \rho_s) BC} \quad (3.2.3.3)$$

$$\phi_D = \phi_C e^{-(\mu_a / \rho_c) t} \quad (3.2.3.4)$$

where

$\phi$	$\gamma$ - ray flux at any point
$\mu_a$	Mass absorption coefficient
$\rho_s$	Density of the soil
$\rho_a$	Density of the concrete
BC	Direct thickness of the soil
t	Thickness of the concrete

The total number of  $\gamma$  - rays deposited in the human body  
inside the citadel can be expressed as (Worst possible  
case)

$$\gamma_{enh} = \phi_d A_h \quad (3.2.3.5)$$

where

$A_h$  The average projected area of an average human being

$$= \left[ \frac{\phi_b}{4\pi y_1^2} \left( e^{-(\mu_a/\rho_s) BC} \right) \right] \left[ e^{(-\mu_a/\rho_c) \cdot t} \right] * A_h \quad (3.2.3.6)$$

Hence, the energy deposited per unit weight of the average person(ergs/grm)

$$\gamma_{enh}/Wt = \frac{(\gamma_{enh})}{W_h} \cdot A * 1.6 E -6 \quad \dots \quad (3.2.3.8)$$

When quality factor(QF) = 1 then,

$$\gamma = \frac{(\gamma_{enh})}{W_h} \cdot A * 1.6 E -6 \quad \dots \quad (3.2.3.9)$$

If the buildup factor for soil and concrete are  $B_s$  and  $B_c$  respectively as calculated by Taylor's method for 8 Mev  $\gamma$  ray energy (which could be the most expected average energy of the  $\gamma$  ray emission in the nuclear explosion then,

$$B_s = A_s \cdot e^{-\alpha_s \mu t} + (1 - A_s) e^{-\beta_s \mu t} \quad (3.2.3.10)$$

and

$$B_c = A_c e^{-\alpha_c \mu t} + (1 - A_c) e^{-\beta_c \mu t} \quad (3.2.3.11)$$

$A_s, A_c, \alpha_s, \alpha_c, \beta_s, \beta_c$  are Taylor's coefficients obtained from the Apex 'D'

Hence, the modified equations for flux after taking Buildup factor in to consideration are

$$\phi_{cm} = B_s \phi_c \quad (3.2.3.12)$$

$$\phi_{dm} = B_c \cdot \phi_d \quad (3.2.3.13)$$

A computer program has been written to solve above mentioned equations iteratively to obtain the minimum depth of burial for various ranges, height of bursts and thicknesses of the concrete

The results plotted are as shown in Figs 3.2.3.2, 3.2.3.3, 3.2.3.4 and 3.2.3.5. The results have been discussed in the succeeding paragraph

### Results and Discussion

This parametric study provides the upper limit of the depth of burial. It is necessary to bury the structure up to this minimum limit to avoid the  $\gamma$  ray exposure, which may cause the harmful effects to the occupants of the complex.

This study reveals that if DOB is more than 6m the structure is completely safe for near surface bursts. But DOBs of 2-6 m is

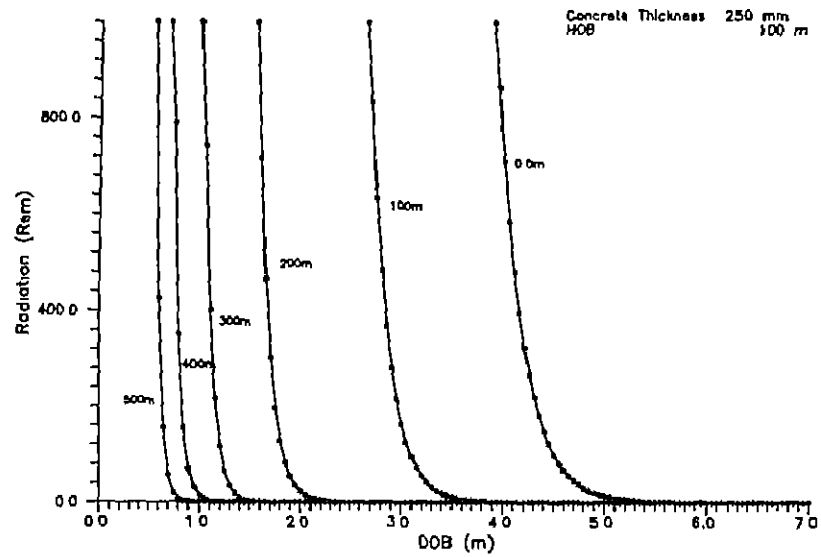


Fig 3.2.3.2 Radiation vs DOB for different Ranges

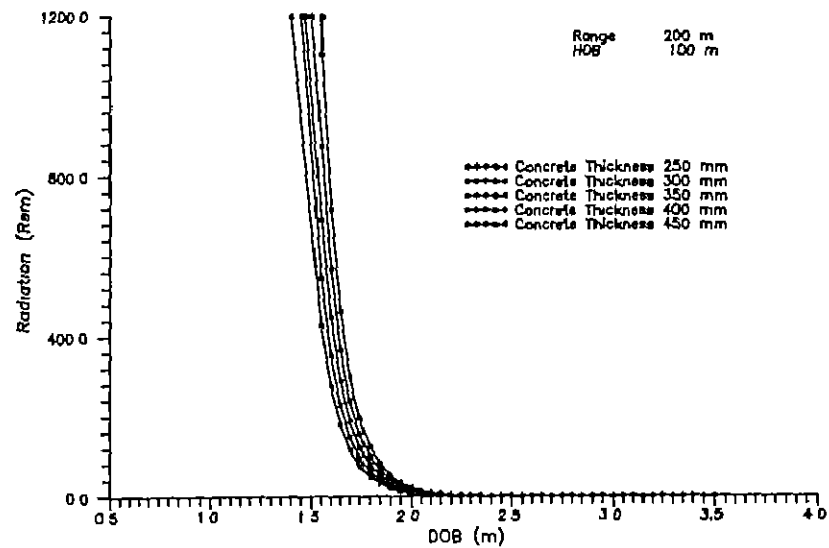


Fig 3.2.3.3 Radiation vs DOB for Various thicknesses of Concrete

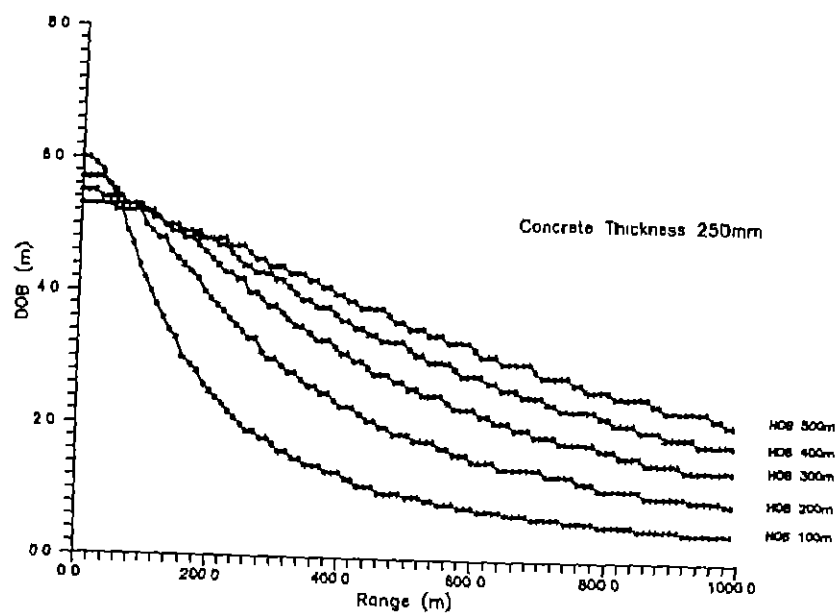


Fig 3.2.3.4 Range vs Optimal DOB

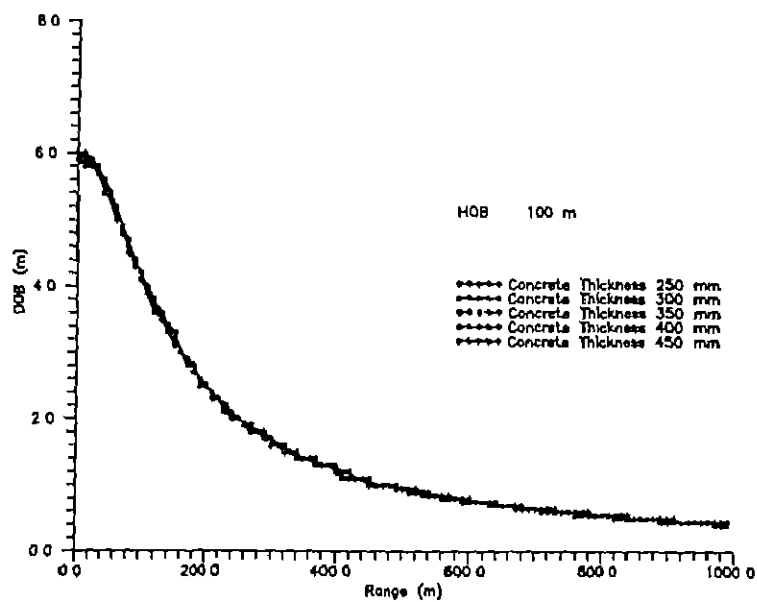


Fig 3.2.3.5 Range vs Optimal DOB for Various Thicknesses of Concrete

sufficient for most possible cases. The concrete is no better than soil as far as radiation absorption is considered and therefore minimum concrete thickness from over pressure considerations should be taken for the analysis. However to start the calculations for radiation a thickness of 250mm may be taken as standard.

#### 3.2.4 Parametric study for Thermal Radiation

Though the thermal radiation does not effect underground construction but it is important to ascertain the safe DOB from its effects. The parametric study performed in the following provides useful results on this aspect. The following assumptions have been made for the analysis.

##### Assumptions

- i) Nuclear explosion source is considered as a perfect black body.
- ii) No atmospheric attenuation is considered.
- iii) Only one third of the total energy of the explosion is associated with direct heat radiation.
- iv) The test results of the Nevada test site, conducted by the United States Department of Defence (USDD) has been taken to obtain the pulse time and other specific details for formulation of the heat radiation.

### Formulation

The fundamental approach adopted to calculate thermal radiation is as given in Fig 3 2 4 1

The approximate duration of the thermal pulse can be obtained in terms of  $t_{\max}$  by the graphs as shown in the Fig 3.2 4 2

where

$$t_{\max} = 0.032 W^{1/2} \text{ s} \quad (3.2.3.1)$$

$W$  weapon yield in kT

The total energy  $E_{\text{tot}}$  emitted in the pulse can be approximated as

$$E_{\text{tot}} = \frac{W}{3} \quad (3.2.3.2)$$

If there is no atmospheric attenuation the thermal energy  $Q$  on the earth surface at a distance  $D$  from the point of the explosion can be given by the following relation. (Fig 3 2 4.1)

$$Q = \frac{E_{\text{tot}}}{4 \pi D^2} e^{-kD} \quad (3.2.3.3)$$

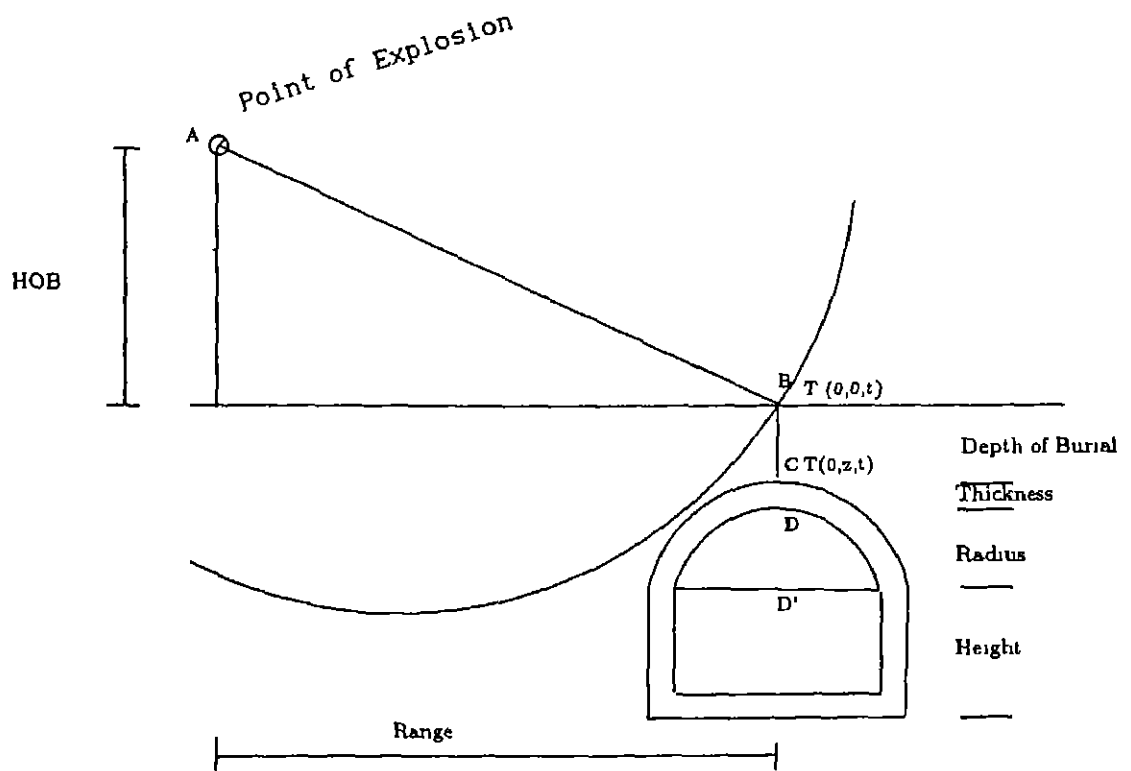


**Fig 3.2.4.1 Thermal Radiation Analysis**

where

\* Absorption coefficient averaged over the whole spectrum of the wavelength

A more useful formulation for thermal energy calculation can be given as

$$Q = \frac{f T W}{4 \pi D^2} \quad (3.2.3.4)$$

where

$f$  The fraction of the total yield in the form of the radiation

$T$  Transmittance, a complex function of the visibility, absorption and the distance Its value can be obtained from Fig 3.2.4.3

The temperature at the earth surface due to the pulse source is governed by the following relation

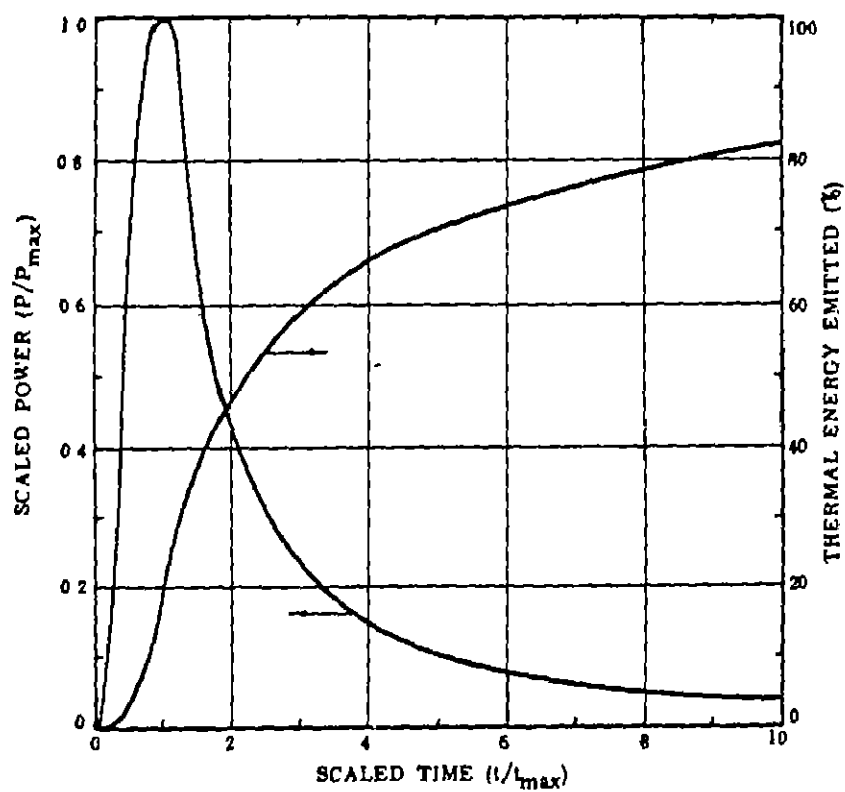


Fig 3.2.4.2 Scaled Time for thermal Pulse

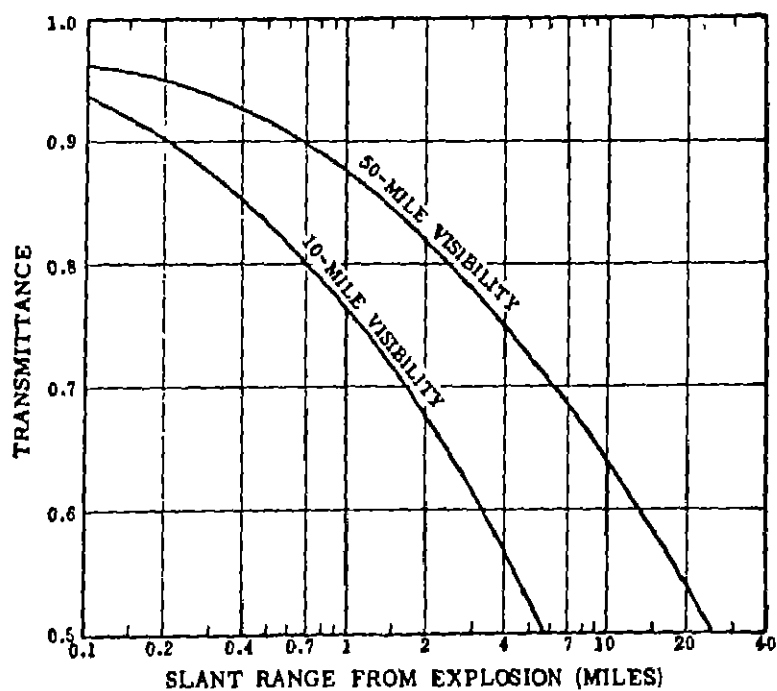


Fig 3.2.4.3 Transmittance

$$T(0,z,t) = \frac{2 I (1-\epsilon)}{\pi \cdot A^2 k} (\alpha t)^{1/2} \cdot \left[ \text{ierfc} \left( \frac{Z}{2(\alpha t)^{1/2}} \right) - \text{ierfc} \left( \frac{(Z^2 + A^2)^{1/2}}{2 (\alpha t)^{1/2}} \right) \right]$$

(3 2 3 5)

where

I	Intensity of the incident thermal energy
A	Area of the source
$\epsilon$	Emissivity of the material
k	Thermal conductivity
$\alpha$	Thermal diffusivity of the material
t	Pulse time

The radiation of this transient temperature with time in atmosphere is given by Stefan - Boltzman law

$$\frac{\delta T_g}{\delta T} = \sigma \epsilon \left[ T_g(t)^4 - T_e^4 \right] \quad (3 2 3 6)$$

where

$\sigma$	Stefan-Boltzman Constant ( 5.56 Watt/m <sup>2</sup> )
$\epsilon$	Emissivity of the soil
$T_g(t)$	Ground temperature in Kelvin at any time
$T_e$	Environment temperature
Z	Depth under consideration

The conduction at any depth is given by the principle of heat conduction through infinite solid medium and can be expressed by the following relation

$$\frac{T_s - T(z,t)}{T_s - T_e} = \operatorname{erfc}\left(\frac{Z}{2(\alpha t)^{1/2}}\right) \quad (3.2.3.7)$$

where

$T_s$	Temperature at the ground surface at any time $t$ in Kelvin
$T_e$	The environment temperature(K)
$T(z,t)$	Temperature at any depth $z$ at any time $t$
$\alpha$	Thermal diffusivity of the soil

A computer program is written and used to obtain the temperature histories at various depths using above mentioned formulation for different ranges & HOBs, for a specific composition of the soil (Apex 'E'). The program assumes the values of some of the parameters as given below

$T$	=	0.9
$f$	=	0.33
$\epsilon$	=	0.93
$k$	=	0.13 W/m.deg
$W$	=	20kT

The Results obtained by varying the other parameters in the equations 3.2.3.6 and 3.2.3.7. The results obtained are plotted as shown in Figs 3.2.4.4, 3.2.4.5 and 3.2.4.6. These are discussed in following paragraph

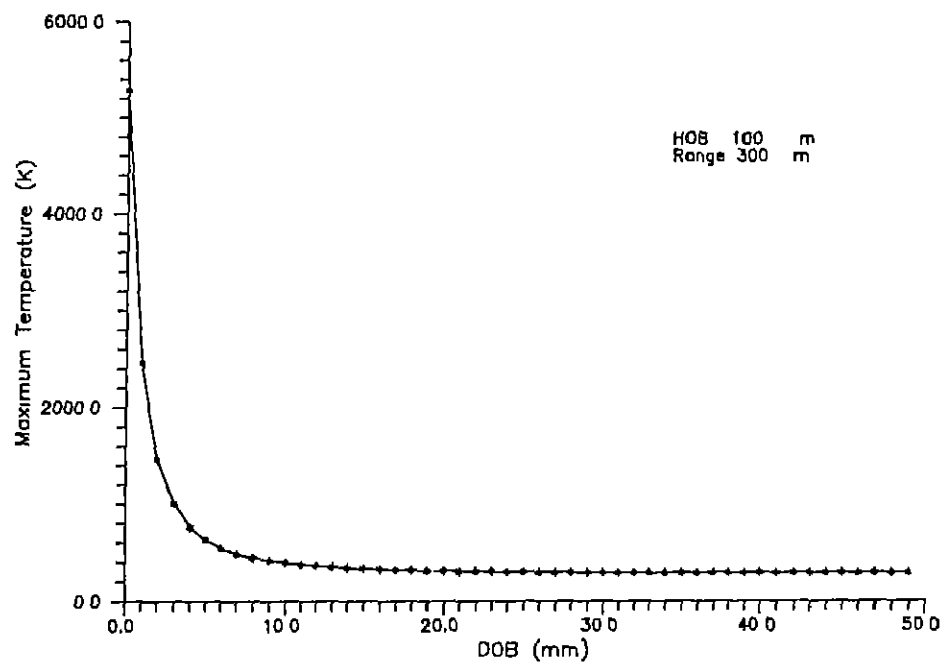


Fig 3 2.4.6 Maximum Temperature vs DOB

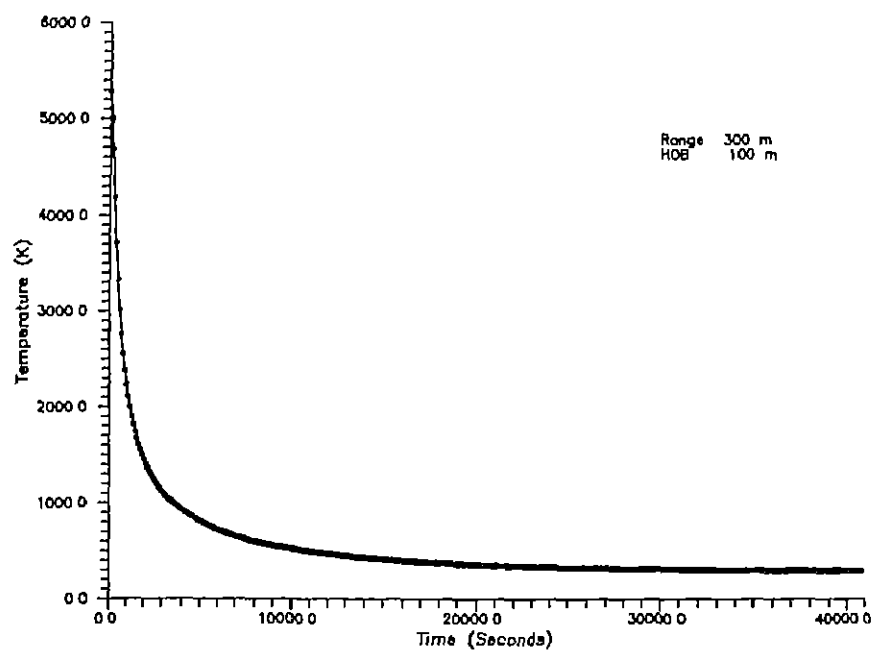


Fig 3 2 4 4 Temperature vs Time at Ground Surface

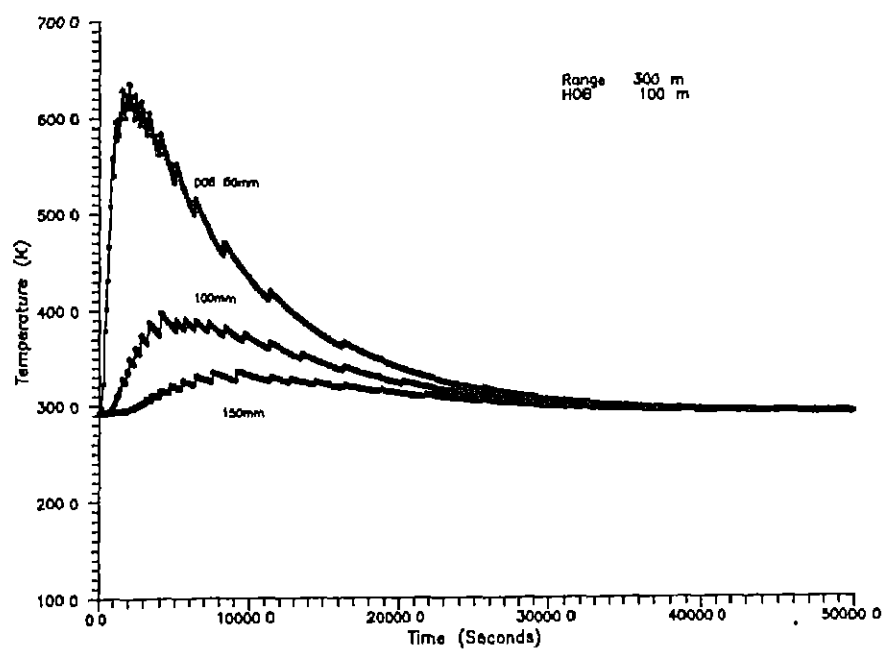


Fig 3 2 4 5 Temperature vs Time for Various Depths

## Results and Discussion

The maximum temperature at any depth may cause thermal expansion of the structural material and is of interest from stress analysis point of view

It is evident that for near surface bursts the temperature on the surface may be as high as  $2000^{\circ}\text{C}$ - $3000^{\circ}\text{C}$  but it decays exponentially. As the heat radiation from the top surface is faster than its conduction through soil layer. Therefore the surface 1000mm below ground virtually remain unaffected. As other forms of radiation requires more DOB for the optimum choice, therefore the thermal radiation is rarely a driver in design. As a rough approximation it can be stated that the DOB more than 1 m is sufficient to protect against the heat radiation for near surface bursts

### 3.3 Pressure - Time History

the pressure time history at the ground surface at any distance from the point of explosion can be obtained from analytical expression as given in Apex 'B'. This provides a scaled output for 1 kT of explosion. Therefore the output available needs to be de-scaled for the magnitudes of interest.

The arrival time and the duration of the positive phase can also be interpreted from the above expression. The value of peak over pressure as input for this expression is calculated from the expression given in Apex 'A'. The time histories at various depths depend on the soil and structure interaction with the blast wave. As

a first approximation the time histories at any depth can be calculated with following assumptions

### Assumptions

- i) The load produced by ground shock on structures buried in a medium with a finite shear strength are influenced by structure medium interaction as the loaded structure deforms, besides by the effects of the propagating transient wave.
- ii) The reflected stress is relieved first by reflections from the concrete air interface at the bottom of the roof.

### Formulation

With these assumptions the loading - time history at any depth can be formulated as follows

The pressure - time history at any given slant range from the point of explosion can be evaluated by the analytical expression as given in Apex 'B'

For  $x \geq x_m$  and  $y \leq 0.38$

$$P_g(x, y, t) = P_g(r, z) \cdot (1+a) \cdot (b \cdot v + c) \quad (3.3.1)$$

and, for  $x < x_m$  or  $y > 0.38$

$$P_s(x,y,t) = P_s(r,z) \quad (b) \quad (3.3.2)$$

where

$P_s(x,y,t)$  Pressure at any time  $t$  for any range  $r$  from the point of explosion

$P_s(r,z)$  Peak over pressure for any range  $r$  from the point of explosion and can be obtained by the analytical expression as given in Apex 'A'

the other variables are as explained in Apex 'B'

The stress at the roof surface at any depth without considering the soil arching relation can be obtained as

$$\sigma_r(t) = P_s(x,y,t) (2 - t/t_d) \quad \text{for } t \leq t_d \quad (3.3.3)$$

$$\sigma_r(t) = P_s(x,y,t) \quad \text{for } t < t_d \quad (3.3.4)$$

If the soil arching is considered then

$$\sigma_r(t) = P_s(x,y,t) \cdot (2 - t/t_d) \quad \text{for } t \leq t_d$$

$$\sigma_r(t) = C_a P_s(x,y,t) \quad \text{for } t < t_d \quad (3.3.5)$$

The stress acting on the side of the shallow buried structure can be given as

$$\sigma_s(t) = K_o \cdot P_s(x,y,t) \quad (3.3.6)$$

If the soil - Arching is considered then

$$\sigma_s(t) = C_a K_o P_s(x,y,t) \quad (3.3.7)$$

where

$$K_o = \frac{1 - \sin \phi}{1 + \sin \phi} \quad (3.3.8)$$

This formulation provides vertical and horizontal pressure time histories acting on the roof and the side of the structure at the desired depth for shallow buried case. As the overburden pressure on the structure constantly acts on the structure, the total vertical  $\sigma_{rtotal}(t)$  and horizontal  $\sigma_{stotal}(t)$  histories can be obtained as

$$\sigma_{rtotal}(t) = \sigma_r(t) + P_{viro} \quad (3.3.9)$$

$$\sigma_{stotal} = k_o \times \sigma_{rtotal}(t) \quad (3.3.10)$$

where

$$P_{viro} = \gamma \cdot DOB$$

A computer program has been written to obtain the loading on the roof and the side of the buried structure for various ranges from the point of the explosion. The time-history obtained for a specific range (distance 300 m and HOB 100 m) and depths are shown in Figs 3.3.1. and 3.3.2 (a) and (b). These have been further used for dynamic analysis of the proposed modules. In addition to the values

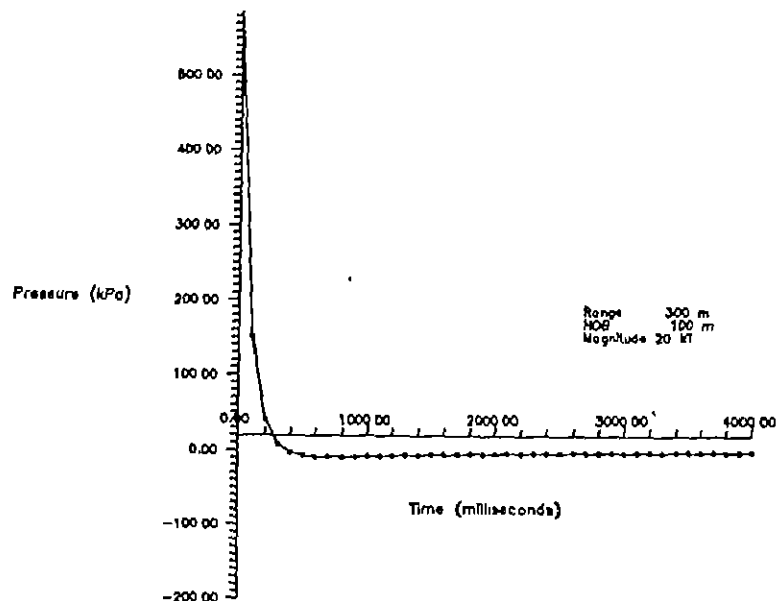


Fig 3.3.1 Surface Pressure - Time History

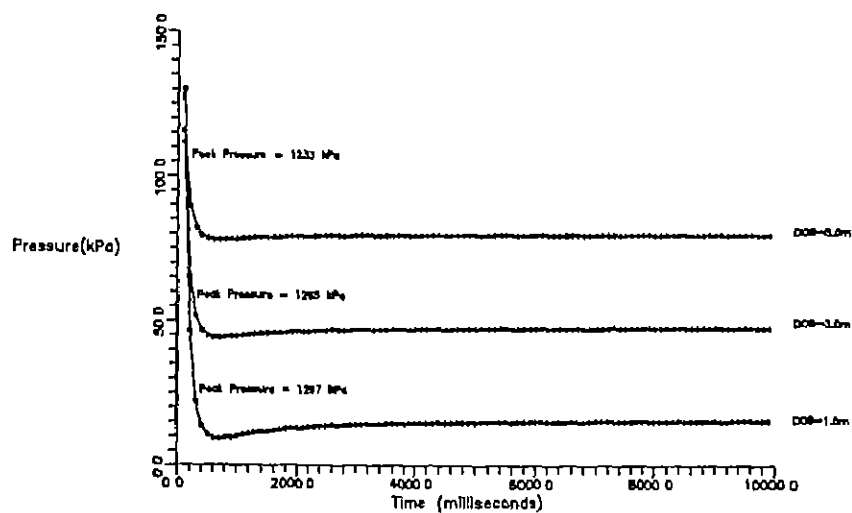


Fig 3.3.2 (a) Vertical Pressure Time History at Various Depths

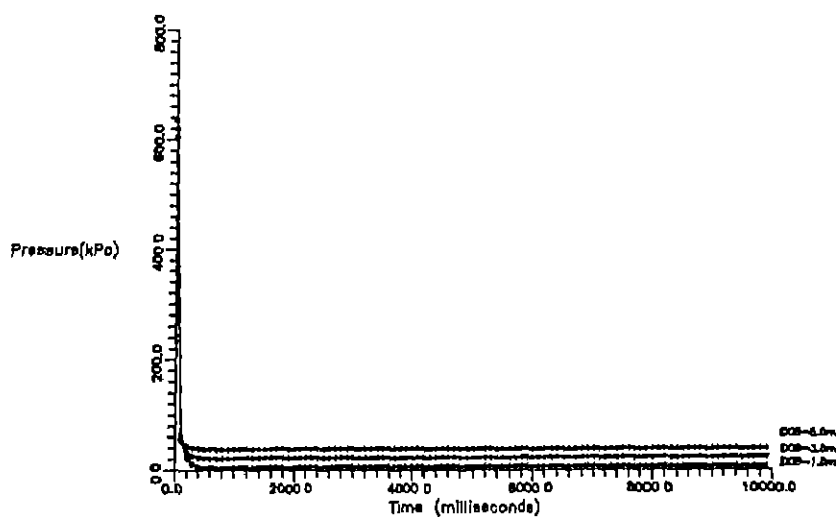


Fig 3.3.2 (b) Horizontal Pressure Time History at Various Depths

of parameters assumed in previous sections the program assumes the value of following parameters as

$$t_d = 12 \quad D / C$$

$$C = 600 \text{ m/s} \quad \text{Compression wave velocity}$$

$$D = 250 \text{ mm} \quad \text{Thickness of the roof}$$

### 3.4 Analysis

The static and dynamic analysis of one of the the principal module of the complex has been performed

The dimensions and other specifications of the module are as shown in Fig 3 4.1

The analysis has been performed for 20 kT explosion at 300m away at 100m HOB

M 20 concrete with density  $24 \text{ kN/m}^3$  has been used for analysis purpose The other assumptions of parametric studies are valid for this analysis.

#### 3.4.1 Load Modeling on the Principal Module

The load modeling of the principal module has been shown in Fig 3.4.2 (a) and (b) for static and dynamic analysis cases The enveloped view of the module has been shown with loading on the elements.

#### 3.4.2 Design Parameters

Based and the parametric studies performed in the previous sections, the design parameters obtained for the static analysis which are given in Table 3.4.2.1

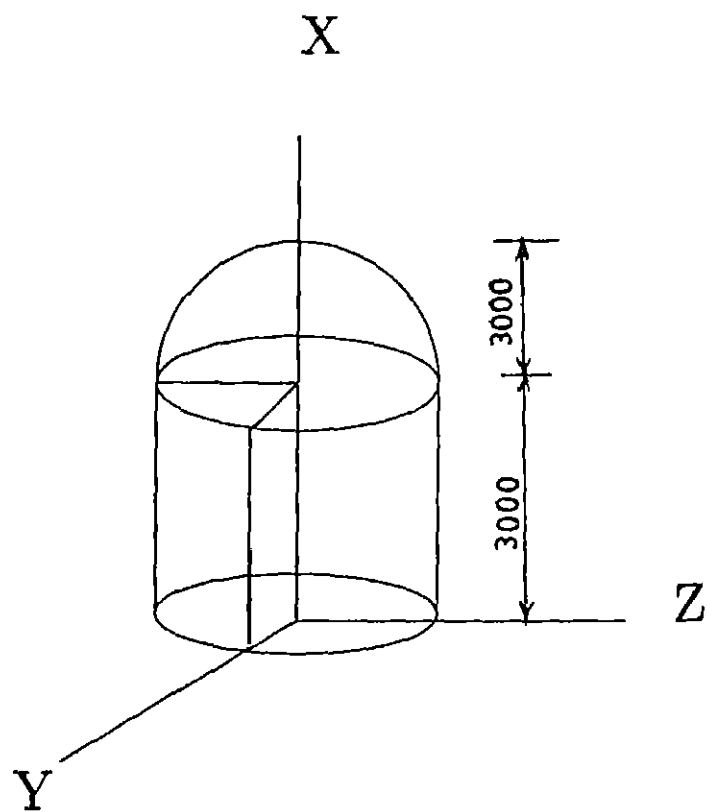


**Fig 3.4.1**      **Outline Diagram of the Principal Module**

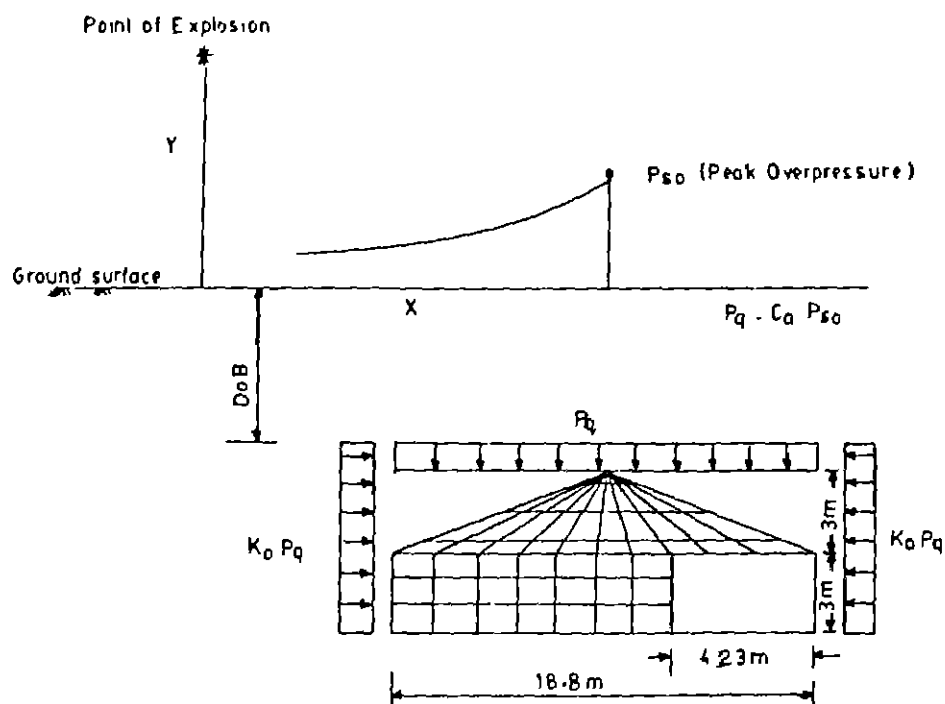


Fig 3.4.2 (a) Load Modeling of the Principal Module for  
Static Analysis

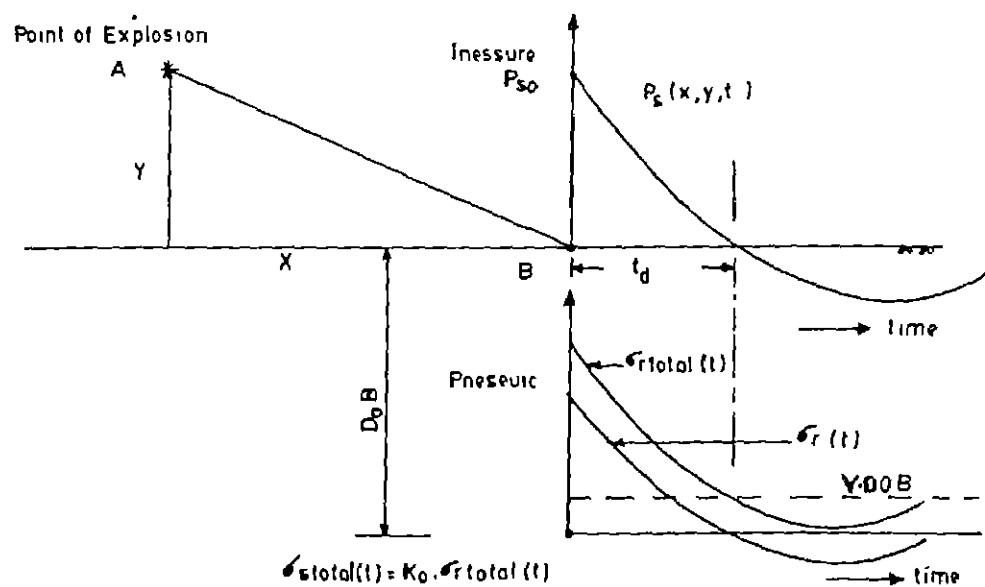


Fig 3.4.2 (b) Load Modeling of the Principal Module for  
Dynamic Analysis

**Table 3.4.2.1 Design Parameters For a Specific Case**

Range = 300m      HOB = 100m      Magnitude = 20 kT

S.No	DOB (m)	Peak Over Pressure (kPa)	Over- Burden Pressure	$\gamma$ - Radiation (Rem)	Thermal (K)
1	2.0	352.3	32.0	0.3	293
2	3.0	280.0	48.0	< 0.3	293
3	4.0	233.0	64.0	< 0.3	293
4	5.0	202	80.0	< 0.3	293

Similarly the vertical and horizontal time histories acting on the structure at 300m range at 4m depth are shown in Fig 3.3.2 (a) and (b). These histories have further been used for dynamic analysis

### 3.4.3 Finite Element Modeling

The suggested module of the complex has been modeled as thin shell elements of arbitrary geometry formed from four compatible triangles. The shell element uses the constant strain triangle. The central node is located at the average of the coordinates of the four nodes. The element has six degrees of freedom which are eliminated prior to the assembly, therefore the resulting quadrilateral element has four degrees of freedom i.e six degrees of freedom at each node

in the global coordinate system.

The bottom nodes are constrained in all the direction and other nodes have degrees of freedom in all the six directions

The openings in the module have been taken care of by providing different element type at the opening with negligible elastic modulus and the same thickness value to maintain the continuity and compatibility

The thermal radiation effects on the structure due to blast have been taken care of by providing the temperatures at nodes according to the results obtained by parametric studies of section 2 2 4

The Global and Elemental coordinate system are as shown in the Fig 3 4 3.1.

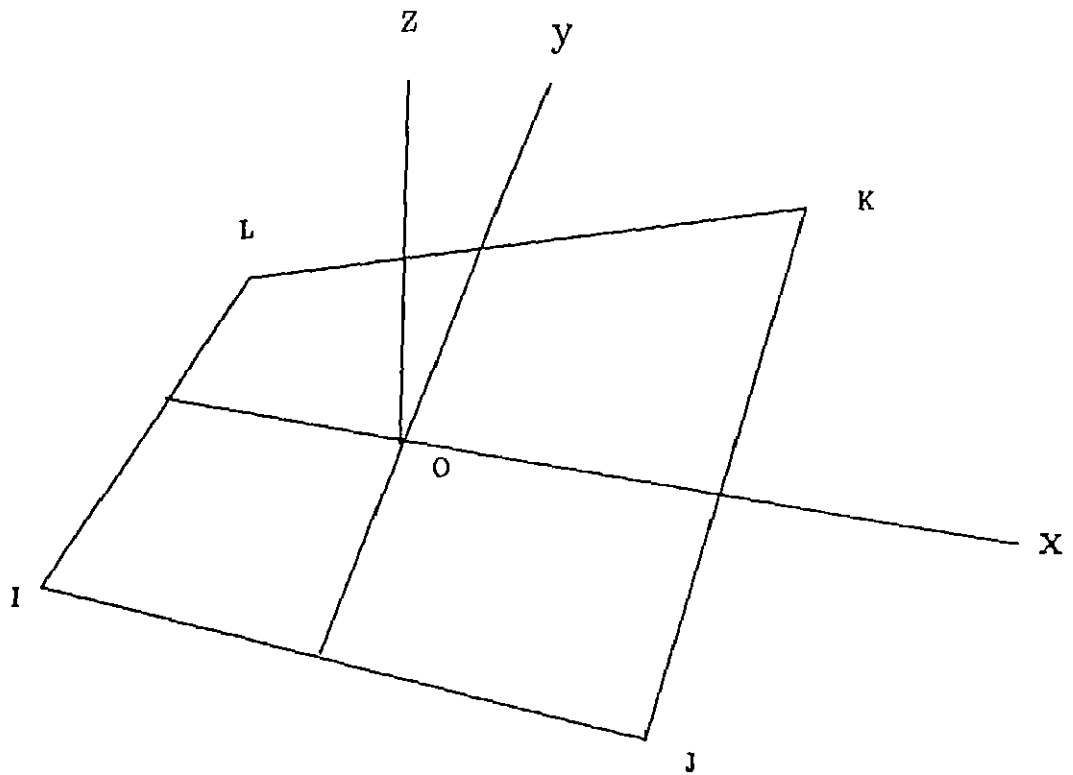
The finite element modeling of the module of the complex are as shown in Fig 3 4 3.2

A preprocessor was developed to provide input to SAP-IV for static analysis The loads on the shell elements act normal to the surface for analysis. The stresses and deflections of all the elements are recovered in output which is of interest for the design The following parametric studies are performed to obtain the desired mesh size for optimal results

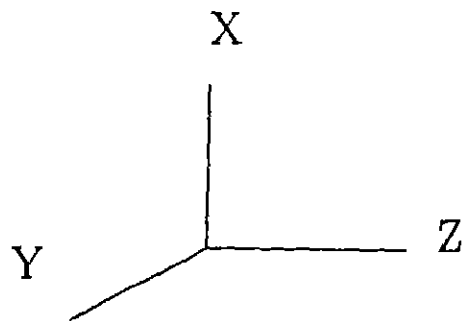
#### 3.4.3.1 Parametric Studies

The following parametric studies have been performed

- i) Stress on any arbitrary chosen element vs size of the mesh (Fig 3 4 3 3)
- ii) Bending moment per unit run on any arbitrary element vs size of the mesh (Fig 3 4.3.4)
- iii) Maximum stress vs size of the mesh



(a) Element Coordinates



(b) Global Coordinates

Fig 3.4.3.1 Elemental and Global Coordinates

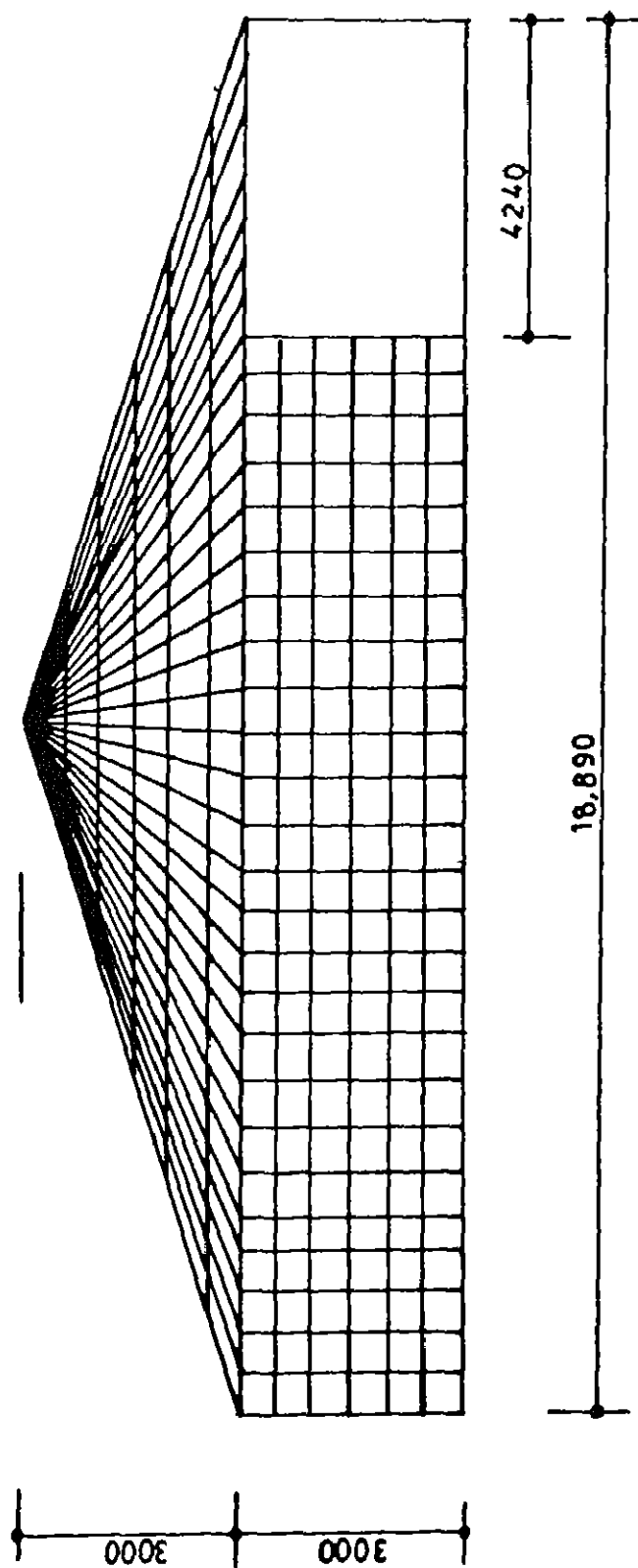


Fig 3.4.4.3.2 Finite Element Modeling of the Principal Module

(Fig 3 4 3 5)

- iv) Maximum bending moment vs size of the mesh  
(Fig 3 4 3 6)
- v) Processor time vs number of elements  
(Fig 3 4 3 7)

### Results and Discussion

The parametric studies performed above for optimal size of the mesh reveals that no of elements should be taken as 1600 - 2000 (250x250mm -200x200mm) for optimum results if the thickness of the model is uniform as 250mm. However, with increasing thicknesses at critical sections for stress reduction demands a fresh parametric study for the optimum results. The element should be kept as square element.

#### 3.4.4 Static Analysis

The parametric studies performed in the foregoing revealed that the openings and the joints of the shells are critical due to stress concentration. Even for the vertical pressure of 200 kPa the stresses on these sections exceeded the critical stresses almost by 200%. Therefore the mesh size was readjusted with increasing thicknesses at these sections (ring beam at the joint of the shells).

The parametric studies were once again performed to obtain the desired results. It was found that the mesh size of 410mmx400mm (585 elements) provides the optimum stresses.

The static analysis performed is performed with this readjusted mesh for various load conditions and varying thicknesses. The results obtained are as shown in Table 3 4 4 1.(a) and (b).

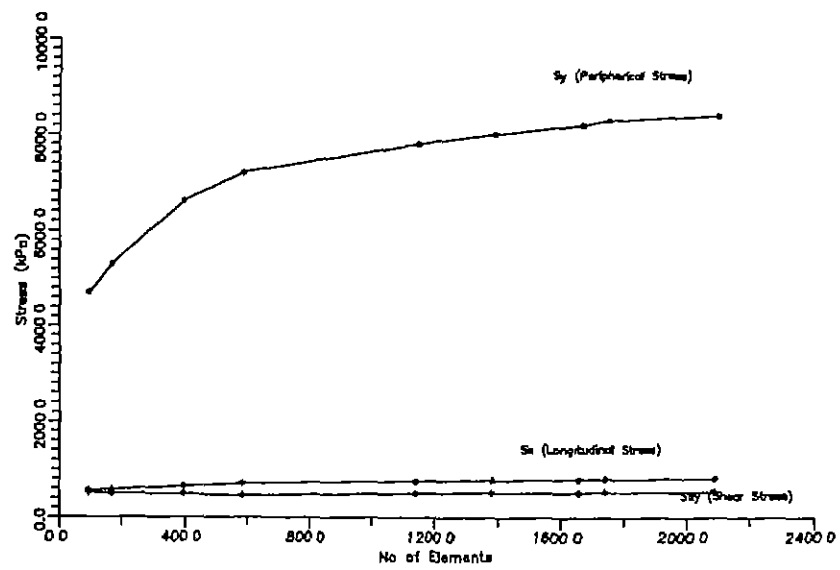


Fig 3 4 3 3 Stress on arbitrary element vs Number of Elements

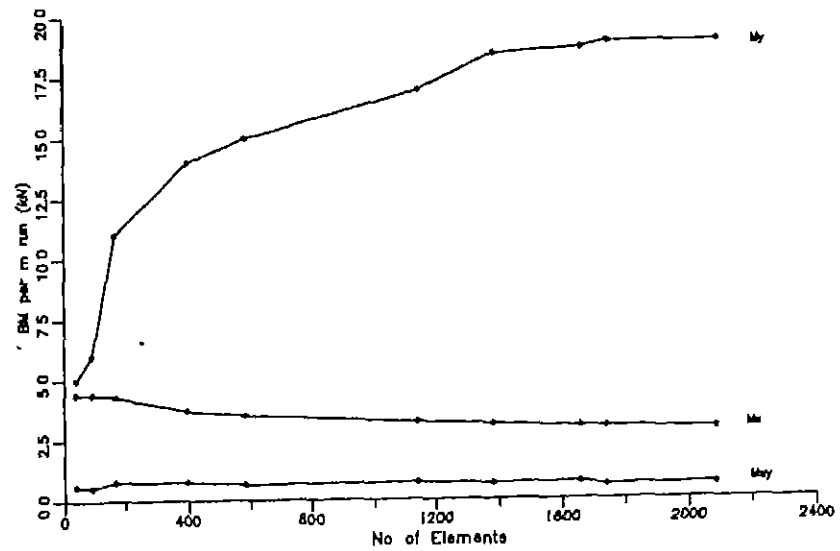


Fig 3 4 3 4 Bending moment on arbitrary element vs Number of Elements

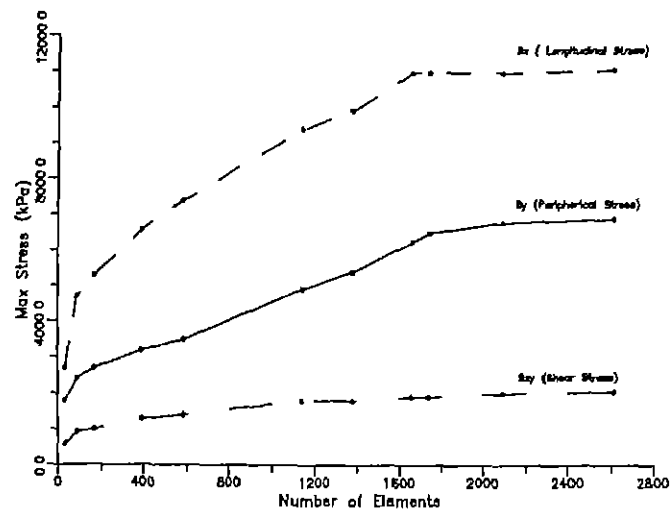


Fig 3.4.3.5 Maximum stress vs Number of Elements

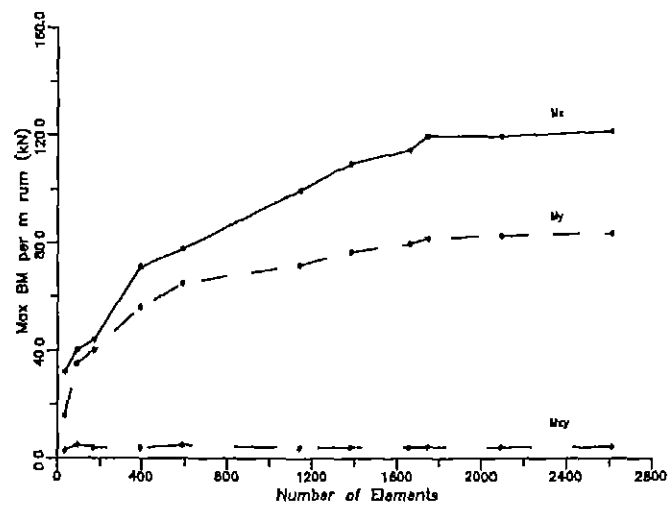


Fig 3.4.3.6 Maximum Bending Moment vs Number of Elements

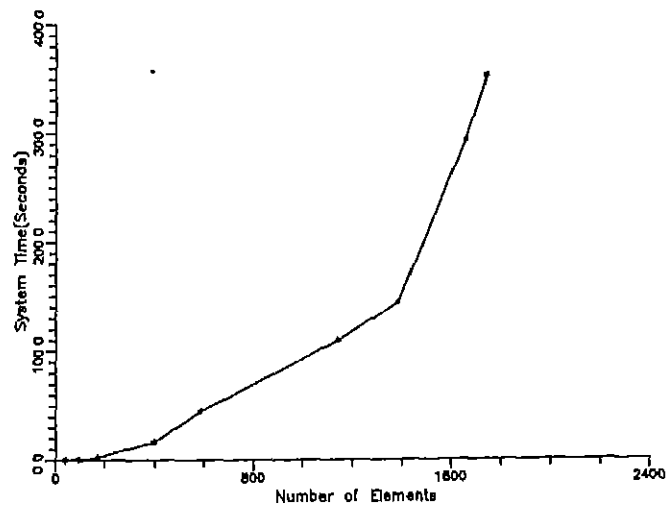


Fig 3.4.3.7 Processor Time vs Number of Elements

Table 3.4.4.1 (a) Results of Static Analysis

S	DOB (m)	Peak over pre ssure (kPa)	Thickness (mm)				Max Stresses (kPa)		
			Cylinder		Dome		S <sub>x</sub>	S <sub>y</sub>	S <sub>xy</sub>
			Near opening cyl (20°)	Rest cyl	Ring beam	Rest dome			
1	2.0	352.3	600	300	400	200	0.15E4	0.36E4	0.63E3
2	2.0	352.3	500	250	300	150	0.20E4	0.41E4	0.67E3
3	2.0	352.3	400	200	200	100	0.27E4	0.52E4	0.10E4
4	3.0	280.0	600	300	400	200	0.13E4	0.32E4	0.62E3
5	3.0	280.0	500	250	300	150	0.16E4	0.36E4	0.64E3
6	3.0	280.0	400	200	200	100	0.21E4	0.45E4	0.79E3
7	4.0	233.0	600	300	400	200	0.13E4	0.30E4	0.63E3
8	4.0	233.0	500	250	300	150	0.13E4	0.33E4	0.64E3
9	4.0	233.0	400	200	200	100	0.18E4	0.40E4	0.67E3
10	5.0	202.0	600	300	400	200	0.13E4	0.29E4	0.63E3
11	5.0	202.0	500	250	300	150	0.13E4	0.31E4	0.64E3
12	5.0	202.0	400	200	200	100	0.15E4	0.37E4	0.67E3

### Results and Discussion

The results obtained for various thicknesses of the module supports the fact that the critical sections are the openings (20° from the opening) and the joint of the shells. Therefore additional thickness are required at the joint in form of ring beam and at the openings. The compressive stresses are the governing stresses for the design of the modules. The maximum deflections in principle directions are as shown in Table 3.4.4.1 (b).

Table 3.4.4.1.(b) Results of Static Analysis

S	DOB (m)	Peak over pre ssure (kPa)	Thickness (mm)				Max Deflections (mm)		
			Cylinder		Dome		X transl- ation	Y transl- ation	Z transl- ation
			Near opening (20°)	Rest cyl	Ring beam	Rest dome			
1	2.0	352.3	600	300	400	200	0.22E-2	0.24E-2	0.22E-2
2	2.0	352.3	500	250	300	150	0.31E-2	0.30E-2	0.31E-2
3	2.0	352.3	400	200	200	100	0.52E-2	0.59E-2	0.50E-2
4	3.0	280.0	600	300	400	200	0.20E-2	0.21E-2	0.20E-2
5	3.0	280.0	500	250	300	150	0.27E-2	0.30E-2	0.27E-2
6	3.0	280.0	400	200	200	100	0.45E-2	0.52E-2	0.43E-2
7	4.0	233.0	600	300	400	200	0.18E-2	0.19E-2	0.18E-2
8	4.0	233.0	500	250	300	150	0.25E-2	0.27E-2	0.24E-2
9	4.0	233.0	400	200	200	100	0.40E-2	0.46E-2	0.39E-2
10	5.0	202.0	600	300	400	200	0.17E-2	0.18E-2	0.17E-2
11	5.0	202.0	500	250	300	150	0.23E-2	0.26E-2	0.23E-2
12	5.0	202.0	400	200	200	100	0.37E-2	0.43E-2	0.36E-2

### 3.4.5 Dynamic Analysis

As a first step to dynamic analysis natural frequencies and the mode shapes are calculated for three different specifications of the structure.

A preprocessor is developed to provide input to SAP-IV. The first and second frequencies obtained for various cases are as shown in Table 3.4.5.1.

### Time History Analysis

For dynamic analysis the same module of the complex is loaded with two time histories acting simultaneously. These histories are the same which were obtained in section 3.3. One of these acts vertically (X-direction) on spherical shell (top dome) for 90s. The other acts horizontally (normal to the surface) on the cylindrical portion of the module for the same time. The horizontal time history has further been resolved in global Y and Z directions for the loading on each element. The force on each element has been provided with the help of time multiplier function in SAP-IV.

The time step has been chosen as 1 s. The damping has been assumed as 2%.

A preprocessor has been developed to provide above mentioned details as formatted input to SAP-IV for time integration.

The load modeling is as shown in Fig 3.4.2 (b).

The maximum stresses, deflections and the corresponding time are recovered as an output and are given in Table 3.4.5.2.(a) and (b).

**Table 3.4.5.1      Natural frequencies of the module for various stiffnesses**

S no	Thickness (mm)				Frequencies (Hz ) B	
	Near open 0 (20 )	Rest cyl -nder	Ring beam	Rest cyl -nder	First	Second
1	600	400	400	200	0.3644E2	0.4361E2
2	500	300	300	150	0.3424E2	0.3842E2
3	400	200	200	100	0.2811E2	0.3099E2

Table 3.4.5 2 (a) Results of Dynamic Analysis

S	DOB (m)	Peak over pre ssure (kPa)	Thickness (mm)				Max Stresses (kPa)		
			Cylinder		Dome		S <sub>x</sub>	S <sub>y</sub>	S <sub>xy</sub>
			Near opening (20°)	Rest cyl	Ring beam	Rest dome			
1	3.0	280 0	600	300	400	200	951.6	1520.0	471 0
2	3 0	280 0	500	250	300	150	1189 0	2030 0	666 3
3	3.0	280 0	400	200	200	100	1641.0	3015 0	1094

Table 3.4.5.2 (b) Results of Dynamic Analysis

S	DOB (m)	Peak over pre ssure (kPa)	Thickness (mm)				Max Deflections (mm )		
			Cylinder		Dome		X transl- ation (m)	Y transl- ation (m)	Z transl ation (m)
			Near opening (20°)	Rest cyl	Ring beam	Rest dome			
1	2.0	280 0	600	300	400	200	0.00142	0 00113	00134
2	2 0	280 0	500	250	300	150	0 00208	0 00189	00226
3	2.0	280.0	400	200	200	100	0.00370	0.00203	.00483

$$R_x = \frac{S_{xstatic}}{S_{xdynamic}} \cong 1.3 \quad R_y = \frac{S_{ystatic}}{S_{ydynamic}} \cong 1.7 \quad R_{xy} = \frac{S_{xystatic}}{S_{xydynamic}} \cong 1.0$$

where  $R_x$ ,  $R_y$ ,  $R_{xy}$  are the ratios of static and dynamic stresses

### Results and Discussion

The comparison of the results of static and dynamic analysis reveal the fact that the static analysis for blast load is over conservative. Therefore the dynamic analysis of these structures are recommended for economy in design of the complex. As the loading on these structures are one time measure, therefore

these structures should essentially remain safe from static overburden pressure

### 3.5 Design of Concrete Shells

Keeping in view the results of the analysis in the foregoing the design of the principal modules have been performed as per Indian Standard Codes of Practice [19,20 and 21]

#### 3.5.1 Design

The moments of resistance of rectangular section based on the assumptions of 37.1 of IS-456(1962) for section without and with compression reinforcement is given in Apex 'E' of the code has been used as a basis of the design. The elements have been assumed as rectangular sections.

The element are checked for critical buckling stresses as per IS.2210(1962). The procedure is rewritten in the succeeding paragraph.

#### 3.5.2 Critical Buckling Stress

Instability in a shell may be caused by

- Local buckling in zones submitted to compressive stresses
- Brazier effect
- Combined effects of bending and torsion

### Cylindrical Shells

The permissible buckling stress in a cylindrical shell may be calculated as follows

$$f_{\text{perm}} = \frac{0.25 F_e}{1 + \frac{F_e}{F_{\text{cr}}}} \quad (3.5.2.1)$$

where

$F_e$             Cube Strength of the concrete at 28 days  
 $F_{\text{cr}}$             Critical stress determined in accordance  
                     with IS 2210(1962)

### Buckling in Doubly Curved Shells

For spherical shells the permissible buckling load per unit area from consideration of elastic stability is given by the following relation

$$P_{\text{perm}} = 0.1 \frac{E d^2}{R^2} \quad (3.5.2.2)$$

where

$E$             Elastic modulus of concrete  
 $d$             Thickness of shell and  
 $R$             Radius of Curvature

### 3.5.3 Yield Criteria

The maximum moment at any corner of any element has been checked by assuming the elements as plate elements. Johnsen's plate theory is thus applied to check the ultimate moments in each element. The principle approach adopted is given below.

Let the reinforcement be placed in two orthogonal directions, one along radial X-axis and the other along the circumferential Y-axis of the shell. Since the reinforcement may not be same in both the directions, the corresponding plastic moments will also differ and the element will be orthotropic with regard to its ultimate strength.

Then the ultimate bending moments can be denoted by  $M_{px}$  and  $M_{py}$  for the positive bending and  $M'_{px}$  and  $M'_{py}$  for negative bending.

Yielding occurs when the bending moment on the cross section with angle  $\alpha$  reaches a certain value. Refer Fig 3.5.3.1

Then according to Johansen's failure theory expressions for lower  $Y_L$  and upper yield  $Y_U$  curves can be given as

$$Y_L \quad M_{p\alpha} = M_{px} \cdot \cos^2 \alpha + M_{py} \cdot \sin^2 \alpha \quad (3.5.3.1)$$

$$Y_U \quad M_{p\alpha} = M'_{px} \cos^2 \alpha + M'_{py} \sin^2 \alpha \quad (3.5.3.2)$$

The yield condition in terms of the components  $M_x$ ,  $M_y$  and  $M_{xy}$  is given

$$M_{\alpha} = M_x \cos^2 \alpha + M_y \sin^2 \alpha + M_{xy} \sin 2\alpha \quad (3.5.3.3)$$

Then the condition to be checked is whether

$$M_{p\alpha} > M_{\alpha} \quad (3.5.3.4)$$

A common computer program has been written to check the buckling stresses and permissible moments at all the corners of each element applying the above principle. As the buckling stress are the governing stresses therefore minimum reinforcement (16mm  $\phi$  250 mm c/c) has been provided in both the principle directions. The stresses obtained from the analysis are well within the permissible limits.

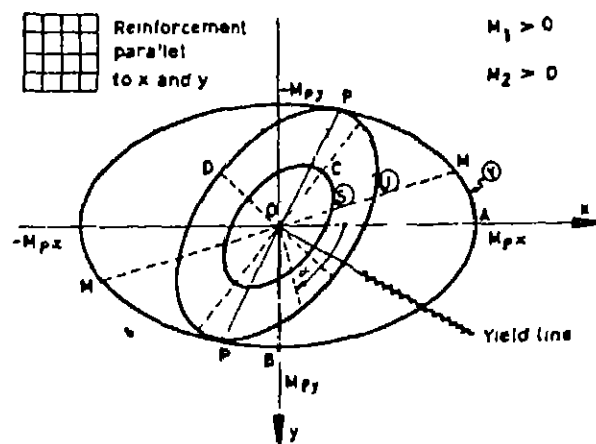


Fig 3.5.3.1 Yield Criteria for shell Elements

## CHAPTER - IV

### CONCLUSIONS

#### 4.1 Suggested Algorithm

The algorithm suggested in section 3.1 incorporates all the effects of nuclear weapon which are governing forces for the design of the complex. The planning, layout and design of the complex has been done as per this algorithm.

#### 4.2 Parametric Studies

The parametric studies performed drive home the following points

i) The probability of the failure of the attacker mission is a function of the dispersal of the facilities and the size of the modules. Therefore the complex should be dispersed to the maximum and the dimensions of the facilities should be as small as possible

ii) Parametric study performed for optimal depth of burial from blast pressure considerations reveals that burying structure deep in the ground is not only uneconomical but it has to be designed for higher soil overburden pressure

iii) The shallow buried structures are advantageous from blast, nuclear and thermal radiation considerations compare to above, mounded , surface flushed and deep buried structures .

iv) The soil cover on the top of the structure is is more economical than the thickness of the concrete from radiation point of view.

v) Upper limit of burial should be based on the radiation considerations.

vi) Although the specialized concretes are available to combat the radiation but the ordinary RCC serves the purpose in present context

vii) It is evident that the thermal radiation is rarely a driver in design but the upper layer of the soil up to one meter depth is susceptible to the thermal radiation Therefore the structures should not be mounded or surface flushed

#### 4.3 Static and Dynamic Analysis

i) The static analysis carried out on the principal shell module supports the fact that the openings and the joints of the shells are critical from the stress concentration point of view. These should be

designed very carefully

ii) The size of the mesh and its refinement with varying stiffness of the elements is important for desired results

iii) The comparison of the static and dynamic stresses reveals the fact that the static analysis for blast force is over conservative. Dynamic analysis should be resorted with taking soil arching into consideration. As the analytical expression for the pressure-time history is approximate, the dynamic analysis with a factor of 1.5 is recommended.

#### 4.4 Scope for future study

The design of structures to resist against nuclear weapon effects is a challenging field for civil engineers. The nations around the world have taken this aspect very seriously in recent years due to nuclear threats.

We may have to construct new structures or upgrade existing construction to cater for these threats which automatically opens new fields for research. The nonlinearity may be increased to obtain more accurate results for these effects. Also, the soil arching relations can be experimentally be found for realistic results.

Apex 'A'

## CALCULATION OF AIR BLAST PEAK OVER PRESSURE

Given

- $x$  scaled range in  $\text{km/kT}^{1/3}$   
 $y$  scaled Height of burst in  $\text{km/kT}^{1/3}$   
 $m$  Magnitude of explosion in  $\text{kT}$

Then

$$r = \left( x^2 + y^2 \right)^{1/2}$$

$$z = y/x$$

Peak over pressure in kPa is given by

$$P_s(r, z) = \beta \left[ \frac{10.47}{(\alpha r)^{a(z)}} + \frac{b(z)}{(\alpha r)^{f(z)}} + \frac{d(z) e(z)}{1 + f(z) (\alpha r)^{g(z)}} + h(z, r, y) \right]$$

in which

$$h(z, r, y) = \frac{-(64.67 z^5 + 2905)}{1 + 441.4 z^5} - \frac{1389 z}{1 + 49.03 z^5} + \frac{8808 z^{1.5}}{1 + 154.5 z^{3.5}} + \frac{.0014(\alpha r)^2}{(1 - .158(\alpha r) + .0486 (\alpha r)^{1.5} + .00128(\alpha r)^2) \cdot (1 + 2 y)}$$

where

$$\alpha = (0.3048)^{-1}, \text{ kft(km)}$$

$$\beta = (100/14.504), \text{ psi (kPa)}$$

$$a(z) = 1.22 - \frac{3.908^2 z}{1 + 810.2 z^5}$$

$$b(z) = 2.321 + \frac{6.195 z^{18}}{1 + 1113 z^{18}} - \frac{03831 z^{17}}{1 + 02415 z^{17}} - \frac{6692}{1 + 4164 \frac{8}{z}}$$

$$c(z) = 4153 - \frac{1149 z^{18}}{1 + 1.641 z^{18}} - \frac{1.1}{1 + 2771 z^{2.5}}$$

$$d(z) = -4.166 + \frac{2576 z^{1.75}}{1 + 1.382 z^{18}} - \frac{8257 z}{1 + 3129 z}$$

$$e(z) = 1 - \frac{.004642 z^{18}}{1 + .003886 z^{18}}$$

$$f(z) = .6096 + \frac{2.879 z^{9.25}}{1 + 2359 z^{14.5}} - \frac{1725 z^2}{1 + 71.66 \frac{3}{z}}$$

$$g(z) = 1.83 + \frac{5.361 z}{1 + .3139 z^6}$$

## ANALYTICAL EXPRESSION FOR PRESSURE - TIME HISTORY

For  $x \geq x_m$  and  $y \leq 0.38$

$$P_s(x, y, t) = p_s(r, z) \cdot (1 + a) \cdot (b v + c) \left( \frac{100}{14.504} \right) \text{ kPa}$$

For  $x < x_m$  or  $y > 0.38$

$$P_s(x, y, t) = p_s(r, z) \cdot (b) \left( \frac{100}{14.504} \right) \text{ kPa}$$

Where

$x$  scaled ground range,  $\text{kft}/\text{kT}^{1/3}$   
 $y$  scaled height of burst,  $\text{kft}/\text{kT}^{1/3}$   
 $t$  scaled time  $\text{msec}/\text{kT}^{1/3}$

$$a = (d - 1) \cdot \left( 1 - \frac{e^{20}}{1 + e^{20}} \right)$$

$$d = 0.27 + \frac{58300y^2}{26667 + 1000000y^2} + 0.27(e) - \left( 0.5 - \frac{0.583000y^2}{26667 + 1000000y^2} \right) e^5$$

$$e = \left| \frac{x - x_m}{x_e - x_m} \right|$$

$$x_m = \frac{170 y}{1 + 337 y^{0.25}} + 0.91 y^{2.5}$$

$$x_e = \frac{3.039}{1 + 6.7 y}$$

$$b = \left[ f \left( \frac{t_a}{t} \right)^g + (1 - f) \left( \frac{t_a}{t} \right)^h \right] \left[ 1 - \frac{(t - t_a)}{d_p} \right]$$

$$t_a = u \quad \text{for } x < x_m$$

$$t_a = u \frac{x_m}{x} + w \left( 1 - \frac{x_m}{x} \right) \quad \text{for } x \geq x_m$$

$$u = \frac{(0.543 - 21.8r + 386r^2 + 2383r^3)r^8}{2.99 \cdot 10^{-14} - 1.91 \cdot 10^{-10} r^2 + 1.032 \cdot 10^{-6} r^4 - 4.43 \cdot 10^{-5} r^6 + (1.632 + 2.629r + 2.69r^2)r^8}$$

$$w = \frac{(1.086 - 34.605r + 486.3r^2 + 2383r^3)r^8}{3.0137 \cdot 10^{-13} - 1.2128 \cdot 10^{-9} r^2 + 4.128 \cdot 10^{-6} r^4 - 1.116 \cdot 10^{-5} r^6 + (1.632 + 2.629r + 2.69r^2)r^8}$$

$$d_p = \left( \frac{1640700 + 24629 t_a + 416.15 t_a^2}{10,880 + 619.76 t_a + t_a^2} \right) * \dots$$

$$\left[ \left( 0.4 + \frac{0.001204 t_a^{1.5}}{1 + 0.001559 t_a^{1.5}} \right) + \left( 0.0426 + \frac{0.5486 t_a^{0.25}}{1 + 0.000357 t_a^{1.5}} \right) (s) \right]$$

$$s = 1 - \frac{1.1 \cdot 10^{10} y^7}{1 + 1.1 \cdot 10^{10} y^7} - \left( \frac{2.441 \cdot 10^{-8} y^2}{1 + 9 \cdot 10^{10} y^7} \right) \left( \frac{1}{4.41 \cdot 10^{-11} + x^{10}} \right)$$

$$f = \left( \frac{0.01477 t_a^{75}}{1 + 0.005836 t_a} + \frac{7.402 \cdot 10^{-5} t_a^{2.5}}{1 + 1.429 \cdot 10^{-8} t_a^{4.74}} - 0.216 \right) \cdot (s) +$$

$$0.7076 - \frac{3.077 \cdot 10^{-5} t_a^3}{1 + 4.367 \cdot 10^{-5} t_a^3}$$

$$g = 10.0 + \left( 77.58 - \frac{64.99 t_a^{0.125}}{1 + 0.04348 t_a^{0.5}} \right) \cdot (s)$$

$$h = 2.753 + \frac{0.05601 t_a}{1 + 1.473 \cdot 10^{-9} t_a^5} + \left( \frac{0.01769 t_a}{1 + 3.207 \cdot 10^{10} t_a^{4.25}} - \frac{0.03209 t_a^{1.25}}{1 + 9.914 \cdot 10^{-8} t_a^4} - 1.6 \right) (s)$$

$$v = 1 + \left( \frac{3.28 \cdot 10^{11} y^6}{1 + 1.5 \cdot 10^{12} y^{6.75}} \right) \left( \frac{g_a^3}{6.13 + g_a^3} \right) \left( \frac{1}{1 + 9.23 e^2} \right)$$

$$c = \left[ \frac{1.04 - \left( \frac{240.9 x^4}{1 + 231.7 x^4} \right) (g_a)^7}{(1+a) [1 + 0.923 (g_a)^{8.5}]} \right] \cdot \left[ \frac{2.3 \cdot 10^{13.9} y^9}{1 + 2.3 \cdot 10^{13.9} y^9} \right] \times$$

$$\left[ 1 - \left( \frac{(t - t_a)}{d_p} \right)^8 \right]$$

$$g_a = \frac{t - t_a}{d_p}$$

$$dt = 474.2 \cdot y \cdot (x - x_m)^{1.25}$$

Here

- xm An approximation to the beginning of mach reflection region
- xe Approximation to the points in the double peak region where the peaks are equal.
- dt Time separation between the first & second peak
- d Ratio of the first peak to second peak
- ta Approximation to the shock arrival time
- dp Approximation to the duration of the positive phase.

Apex 'c'

## Clinical Effects of Ionizing Radiation Doses

Effect/Phase (1)	DOSE/RANGE					
	0 to 100 rems— subclinical range (2)	100 to 1,000 Rems— Therapeutic Range			Over 1,000 Rems— Lethal Range	
		100 to 200 rems— clinical surveillance (3)	200 to 600 rems— therapy effective (4)	600 to 1,000 rems— therapy promising (5)	1,000 to 5,000 rems— therapy palliative (6)	Over 5,000 rems— therapy palliative (7)
Incidence of vomiting	None	100 rems infrequent 200 rems common	300 rems 100%	100%	100%	100%
Initial phase Onset	—	3 to 6 hr	½ to 6 hr	¼ to ½ hr	5 to 30 min	Almost immediately <sup>b</sup>
Duration	—	≤ 1 day	1 to 2 days	≤ 2 days	≤ 1 day	
Latent phase Onset	—	≤ 1 day	1 to 2 days	≤ 2 days	≤ 1 day <sup>a</sup>	Almost immediately <sup>b</sup>
Duration	—	≤ 2 wk	1 to 4 wk	5 to 10 days	0 to 7 days <sup>a</sup>	
Final phase Onset	—	10 to 14 days	1 to 4 wk	5 to 10 days	0 to 10 days	Almost immediately <sup>b</sup>
Duration	—	4 wk	1 to 8 wk	1 to 4 wk	2 to 10 days	
Leading organ	Hematopoietic tissue				Gastrointestinal tract	Central nervous system
Characteristic signs	None below 50 rems	Moderate leukopenia	Severe leukopenia; purpura, hemorrhage, infection Epilation above 300 rems		Diarrhea; fever, disturbance of electrolyte balance	Convulsions, tremor, ataxia, lethargy
Critical period postexposure	—	—	1 to 6 wk		2 to 14 days	1 to 48 hr
Therapy	Reassurance	Reassurance, hematologic surveillance	Blood transfusion, antibiotics	Consider bone marrow transplantation	Maintenance of electrolyte balance	Sedatives
Prognosis	Excellent	Excellent	Guarded	Guarded	Hopeless	
Convalescent period	None	Several wk	1 to 12 mo	Long	—	
Incidence of death	None	None	0 to 90%	90 to 100%	100%	
Death occurs within	—	—	2 to 12 wk	1 to 6 wk	2 to 14 days	< 1 day to 2 days
Cause of death	—	—	Hemorrhage, infection		Circulatory collapse	Respiratory failure, brain edema

<sup>a</sup> At the higher doses within this range there may be no latent phase<sup>b</sup> Initial phase merges into final phase, death usually occurring from a few hours to about 2 days, this chronology is possibly interrupted by a very short latent phase.

Apex 'D'

## TAYLOR'S METHOD FOR CALCULATION OF BUILDUP FACTORS

Taylor's formula for calculation of buildup factor is

$$B = A.e^{-\alpha\mu t} + (1 - A)e^{-\beta\mu t}$$

Where values of  $A$ ,  $\alpha$ ,  $\beta$  for exposure buildup factor data for ordinary Concrete & soil of the composition given in Apex 'E' are given in the Tables below

## For Ordinary Concrete

Photon Energy Mev	A	$\alpha$	$\beta$
0.5	12.5	-0.110	0.010
1.0	10.0	-0.088	0.029
2.0	6.3	-0.069	0.058
4.0	3.9	-0.059	0.079
6.0	3.1	-0.059	0.083
8.0	2.7	-0.056	0.086
10.0	2.6	-0.050	0.084

## For soil

0.5	70.0	0.0754	-0.0471
1.0	20.6	0.0653	0.0224
2.0	9.67	0.0538	0.0599
4.0	6.5	0.0388	0.0690
6.0	5.2	0.0357	0.0675
8.0	3.5	0.0421	0.0920

Apex 'E'

## SOIL COMPOSITION

S No	Element	Percentage
1	Si	28.1
2	Al	8.24
3	Fe	5.09
4	Mn	0.00
5	Ti	0.00
6	Ca	3.65
7	Mg	2.11
8	K	2.64
9	Na	2.84
10	P	0.00
11	S	0.00
12	C	0.00
13	H	0.00
14	O	47.33

REFERENCES

- 1 ASCE Manuals & Reports on Engineering Practice No-42 'Design of Structures to Resist Nuclear Weapons Effects', 1987, ASCE New York
- 2 Samuel Glasstone, 'The Effects of Nuclear Weapons', Revised Edition-1964, United States Atomic Energy Commission, April-1962
- 3 Manual of Corps of Engineers U S Army, 'Design of Structures to Resist the effects of Atomic Weapons' Headquarters department of Army 1965, EM-1110-345-413 Weapon Effects Data
- 4 Kenny G.F, Graham K.J, 'Explosive Shocks in Air' 1985 New York
5. Chilton A B, Shultis J.K and Faw R.E, 'Principles of Radiation Shielding 1984, Prentice Hall, Eagle wood cliffs, New Jersey
6. Kaplan M.F 'Concrete Radiation Shielding' 1989, Concrete Design and Construction Series, John Wiley Sons, Inc, New York
7. Jaeger R.G (ed.) 'Engineering Compendium of Radiation Shielding', 1968-1975, Vol II, Springer Verla New York
8. Harvey E. White, 'Modern College Physics', Fifth Edition

- 1965, D Van Nostrand Company Inc. East-West Press Private Ltd, New Delhi
- 9 Carslaw H S, Jager, 'Conduction of Heat in Solids' 1973 Second Edition, Oxford Clarendon Press, Great Britain
  10. Manfred R Hausmann, 'Engineering Principles on Ground Modifications'
  11. Manual of Corps of Engineers U S Army, 'Design of Structures to Resist the effects of Atomic Weapons', Headquarters department of Army, 1965, EM - 1110 - 345 - 421 Buried & Semi Buried Structures
  12. Wilson D. Stainley, Sibley E A 'Ground Displacement from Air Blast loading', 1962, ASCE Journal (SMFE Division) vol-88, SM6
  - 13 Yu-Ao-He, Tianjin University, 'Soil Structure Interaction Under Blast Loading, China 1985, 'Proceedings of Second Symposium on 'The interaction of Non Linear Munitions with Structures, Florida, April 1985.
  14. J L Darke & J R Britt 'Propagation of Short Duration of Air Blast into Protective Structures' 'Proceedings of Second Symposium on 'The Interaction of Non Linear Munitions with Structures, Florida, April 1985.
  15. Manual of Corps of Engineers U S Army, 'Design of Structures

to Resist the effects of Atomic Weapons' Headquarters  
 department of Army 1965 EM - 1110 - 345 - 420 Arches &  
 Domes

16. Dr B Chatterjee 'Theory & Design of Concrete Shells'
17. S P Timoshenko, L.N.Goodier 'Theory of Plates & Shells'  
 1951, McGraw-Hill New York
- 18 Klaus Juergen Bathe, Edward.L Wilson & Fred Peterson  
 'Structural Analysis Program - IV, 1973, University of  
 California
19. IS:456 (1978), 'Code of Practice for Plain & Reinforced  
 Concrete' Sep 1981, BIS, New Delhi
20. IS: 4991(1968) 'Criteria for Blast Resistant Design of  
 Structures for Explosion Above Ground' 1968, ISI, New Delhi
- 21 IS:2210(1962), 'Criteria for Design of Concrete Shell  
 Structures', 1973 ISI, New Delhi
22. M.A.Save & C.E.Massonet, 'Plastic analysis & Design of  
 Plates, Shells & Disks' 1972, North - Holland Publishing  
 Company, Amsterdam

9121377

CE-1995-M-SHA-PLA



A121377